The "Coulomb Phase" in Frustrated Systems

Christopher L. Henley

Department of Physics, Clark Hall, Cornell University, Ithaca, New York 14853-2501; email: clh@ccmr.cornell.edu

Annu. Rev. Condens. Matter Phys. 2010. 1:179–210

First published online as a Review in Advance on June 10, 2010

The *Annual Review of Condensed Matter Physics* is online at conmatphys.annualreviews.org

This article's doi: 10.1146/annurev-conmatphys-070909-104138

1947-5454/10/0810-0179$20.00

Abstract

The "Coulomb phase" is an emergent state for lattice models (particularly highly frustrated antiferromagnets), which have local constraints that can be mapped to a divergence-free "flux." The coarse-grained versions of this flux or polarization behave analogously to electric or magnetic fields; in particular, defects at which the local constraint is violated behave as effective charges with Coulomb interactions. I survey the derivation of the characteristic power-law correlation functions and the pinch points in reciprocal space plots of diffuse scattering, as well as applications to magnetic relaxation, quantum-mechanical generalizations, phase transitions to long-range-ordered states, and the effects of disorder.

1. INTRODUCTION

1.1. The Basic Idea

A class of interesting lattice systems in solid state physics and statistical mechanics have ground states, which (to a first approximation) are highly constrained yet highly degenerate—that is, more or less, the current definition (1) of a "highly frustrated" magnet. A fundamental problem in handling such systems theoretically is that of "navigation" among these states. Is there a way to label and enumerate the states so as to carry out a sum over them, and evaluate a partition function? Or if a particular state is somehow to be "selected" out of the ensemble—for example, the classical state which optimizes the energy gain from some perturbation term in a classical Hamiltonian, or from quantum fluctuations in a quantum Hamiltonian—how do we find that "needle in a haystack"?

One of the standard answers is a coarse-graining that discards most of the information in the configurations and keeps local averages of certain quantities, thereby converting the lattice problem into a continuum model. For this to be fruitful (and physically meaningful) the quantity being averaged ought to be conserved. (It might also be the order parameter of some long-range order, but our models are liquid-like in the first approximation—that is just paraphrasing the characterization in the first sentence.) In ordinary (off-lattice) liquids, this is rather mundane (local particle densities and momentum densities). But in the lattice models I have in mind, we are back in the wilderness: the microscopic degrees of freedom (e.g., spins) usually do not have a conservation law, and (it being a lattice model) there is no momentum conservation.

Fortunately, in quite a few cases, another kind of conservation is hidden in the first-order ensemble: a constraint on the total spin (or other degree of freedom) surrounding each lattice point. That allows us to map each microstate of local variables into a configuration of (weighted) arrows living on the bonds of the lattice, such that the signed sum of the arrow weights into every vertex (outwards minus inwards) is exactly zero in any allowed configuration. Such arrows are called "lattice fluxes," for this is exactly the zero-divergence condition an electric or magnetic flux would satisfy (in the absence of sources), if the field were constrained to lie along those lattice edges and its flux could only take discrete values.

The desired emergent vector field $\mathbf{P}(\mathbf{r})$ is the coarse-graining of this flux (2–5), i.e., the mean value of the lattice fluxes over a volume centered at $\mathbf{r}$ much bigger than a lattice constant, but much smaller than the system size. Correspondingly, the divergence condition becomes $\nabla \cdot \mathbf{P}(\mathbf{r}) = 0$. Furthermore, it turns out (Section 3) that the effective coarse-grained free energy has the form $\int d^d\mathbf{r} \frac{K}{2} |\mathbf{P}|^2$, exactly the form of the field energy of an electric (or magnetic) field.

There are many ways to apply this analogy to find the long-distance behaviors of our constrained model. Because the probabilities according to this free energy are Gaussian, one can compute practically any desired expectation. In particular, the "spin" correlations depend on separation R with the functional form of a dipole-dipole interaction, proportional to $1/R^d$ in d dimensions. It was somewhat surprising to find such a slow decay (with a divergent correlation length) in such a liquid-like, maximally random system. Such states (in three dimensions) have acquired the name "Coulomb phase."

The conditions for a Coulomb phase are the following:

C1: Each variable can be mapped to a signed flux $\mathbf{P}_i$ running along bond i;
C2: the variables obey hard constraints, such that the sum of the (incoming) fluxes at each (parent) vertex is zero; and
C3: the system is in a highly disordered phase, without any long-range-ordered pattern. This may be called "liquid-like" to express the disorder coupled with strong local correlations (implicit in C2).

1.2. Rearrangements

What local rearrangements are permitted by the flux constraint? If I flip the variable on a bond adjacent to parent lattice site α, so as to change its flux from incoming to outgoing, I must flip the flux in the opposite way on one of the other bonds. Thus, the natural rearrangements (either in a simulation or a real system) are entire *loops*, which are sometimes called "Dirac strings." As one traverses the string in a particular direction, the sense of the flux arrows is always the same with respect to the walking direction; the local rearrangment reverses this sense, from always forward to always backward or vice versa. Thus, if the string extends across the whole system, the rearrangement changes **P**, but if the string closes, then **P** is unchanged. (An example of such an update is shown later in **Figure 4*a***.)

1.3. Overview

The aim of this review is to survey the lattices and models (and real materials) in which a Coulomb phase is found (Section 2), to walk through the derivation of its power-law correlations (Section 3), and to highlight some interesting ways that Coulomb-phase ideas have been deployed to solve problems in frustrated systems. These include topological defects that (in the case of dipolar spin ice) are (emergent) *magnetic monopoles* (Section 4), dynamics (Section 5), quantum-mechanical generalizations (Section 6), transitions to ordered phases (Section 7), and quenched disorder (Section 8).

Although this review touches on many aspects of frustrated spin models (gauge theories, disorder, quantum dimer models, dynamics), it does not aim or claim to review any of these major topics, except for particular instances that happen to be tractable using the Coulomb-phase notions. Indeed, even concerning the Coulomb-phase developments to date, I have not tried to exhaustively survey all papers; I only try to represent each aspect of the topic in the sections listed above. My choice of particular results to highlight is driven by the motive of presentation, and does not always imply priority or importance.

2. EXAMPLES

How can we realize a Coulomb phase? This breaks up into two questions: which *models*, on which lattices, have the requisite constraints (Section 2.1), and which *physical* systems realize such models (Section 2.2–2.5)? Of course, though two physical systems may realize mathematically equivalent models, quite likely, different kinds of quantities are experimentally accessible in the respective systems.

I also point out that one might view the constrained system as either a $T = 0$ or $T = \infty$ limit of some statistical mechanics model. On the one hand, if we consider an enlarged configuration space in which the constraint is not forced, but its violation costs energy (as I do in Section 4), the constrained model is the $T = 0$ limit. On the other hand, within

the constrained ensemble, we might consider adding a Hamiltonian, which breaks the degeneracy among states—examples are kagomé ice (Section 2.5.1) and the perturbations driving transitions in Section 7—in which case the basic ensemble is the $T = \infty$ limit.

2.1. Lattices

What models give rise to Coulomb phases? First, I talk about the lattices, and then the degrees of freedom.

2.1.1. Parent and medial lattices. First of all, we always have a "parent" lattice $\mathcal{B}$, which is bipartite, i.e., one that can be partitioned into (equivalent) sublattices of even and odd nodes such that every bond connects an even node to an odd node. Degrees of freedom—which I call "variables" for short—live on these bonds, i.e., on sites of "medial" lattice $\mathcal{L}$ defined to consist of the bond midpoints. (I call sites of the parent lattice "nodes," simply to distinguish them from "sites" of the medial lattice.)

Conversely, I call $\mathcal{B}$ the "premedial" lattice of $\mathcal{L}$. In the literature, $\mathcal{B}$ is often sloppily called the "dual" lattice, which properly means something different. For example, the premedial lattice of the kagomé lattice is the honeycomb, but the dual of the kagomé lattice is the dice lattice.

The most important three-dimensional example is the pyrochlore lattice (diamond as parent lattice) (see **Table 1**). The simplest realization is the "*B*" sublattice (octahedral sites) of the spinel (usually oxide) structure. The other important realization is the pyrochlore crystal structure. (This is adopted by a large family of oxides, which contain *two* interpenetrating pyrochlore lattices, each occupied by a different species of cation.)

An example which deserves more attention is the "half-garnet" lattice. The magnetic lattice in a garnet consists of two interpenetrating copies of this lattice. [The "hyperkagomé" lattice (14, 15) is equivalent to the half-garnet lattice—so long as only first-neighbor bonds are taken into account—but has less symmetry: one primitive cell of hyperkagomé is two primitive cells of half-garnet.] The parent lattice is the "Laves graph of

Table 1 Parent lattices and medial lattices. The table shows the spatial dimension d, the parent lattice with its coordination $Z_{\mathcal{B}}$, the Bravais lattice, the medial lattice with its coordination $Z_{\mathcal{L}}$, and the number of sites per cell. The length ℓ_{loop} of the shortest loop (same in either lattice) is also given. Finally, a reference for the lattice is given. The clusters formed around each node of the parent lattice have $Z_{\mathcal{B}}$ sites (forming triangles, tetrahedra, or octahedra).

d	Parent lattice $\mathcal{B}$	$Z_{\mathcal{B}}$	Bravais lattice	Medial lattice $\mathcal{L}$	$Z_{\mathcal{L}}$	Sites/cell	ℓ_{loop}	Ref.
2	Square	4	Square	Checkerboard	6	2	4	6, 7
	Honeycomb	3	Triangle	Kagomé	4	3	6	
	4–8 lattice	3	Square	"Squagome"	4	4+2	4	8
	Diamond bilayer	3,4	Triangle	"Kagomé sandwich"	5,6	7	6	9
3	Simple cubic	6	Simple cubic (sc)	Octahedral	8	3	4	10–12
	Diamond	4	Face-centered cubic (fcc)	Pyrochlore	6	8	6	
	Laves graph	3	Body-centered cubic (bcc)	Half-garnet	4	4	10	13

degree three," in which each vertex has three bonds forming 120° angles, and its Bravais lattice is bcc; thus, its symmetry is just as high as the pyrochlore's.

I also include the "octahedral" lattice, which gets reinvented from time to time as a toy model because its parent lattice is simple cubic, suitable for simple-minded theorists. Finally, the "sandwich" lattice consists of two kagomé layers linked by an additional triangular layer, and models the antiferromagnet $SrCr_{8-x}\ Ga_{4+x}O_{19}$; thus, it is essentially two dimensional. There are experimental realizations for most of these lattices.

For pedagogical purposes, I use two-dimensional lattices in all figures, even though these are *not* quite bona fide Coulomb phases (see Section 3.3). The reader should view them somewhat more as analogies (to $d = 3$) rather than as examples.

2.1.2. Degrees of freedom. The most common models reduce to either ice models or dimer models. An ice model is defined on a parent lattice with even coordination number $Z_{\mathcal{B}}$ (also called a "six-vertex" model in the usual case $Z_{\mathcal{B}} = 4$). Every edge carries an arrow, and at every vertex the "ice rule" constraint is obeyed; namely, half the vertices point in and half point out (16, 17). This arrow obviously *is* the flux. (See **Figure 1*a***.)

A dimer means an object that covers two nodes of the parent lattice. Unless otherwise specified, a dimer covering also satisfies the condition that every node is covered by *exactly* one dimer: dimers never overlap, and no node is left uncovered. To define the flux, we draw an arrow of weight $Z_{\mathcal{B}} - 1$ along each dimer-occupied edge, pointing from the even to the odd node, and arrows of weight 1 along each unoccupied edge, pointing in the opposite direction. (Obviously a different overall normalization of the flux could be used.) Illustrations of this weighting may be found later in **Figure 5*a,b,d***.

2.2. Water Ices

I now turn to the different kinds of physical realization, starting with real ice. In crystalline H_2O, the O atoms form a diamond lattice with hydrogen bonds to all four neighbors.[1] Two of the these adjacent H's are covalently bonded to the O in question (as H_2O), whereas the other two H's belong to the neighboring O's (see **Figure 1*b***). The variables representing a configuration of the H's are arrows along the lattice bonds and clearly satisfy the "ice rule." This is the first highly frustrated model to be analyzed by Bernal & Fowler (16) and Pauling (17) in the 1930s.

There are many structures (often ferroelectrics) having hydrogen bonds such that the low-energy structures realize some kind of ice rules.

2.3. Lattice-Gas Orders

An important way to realize constraints is when some kind of mutually repelling particle occupies the medial lattice sites. If we constrain the overall filling n by these particles to certain rational fractions, and if the interactions are only nearest neighbor, it is easy to see that the ground states are those in which *every* triangle or tetrahedron has the same filling. If we have two species A and B that attract each other more than their own kind, with filling n of species A and $1 - n$ of species B, as suggested for $CsNiCrF_6$ (18, 19), we get

[1]The usual form of water ice uses the hexagonal diamond lattice. The cubic diamond lattice used in the model has very similar behaviors, but is nicer theoretically owing to its higher symmetry.

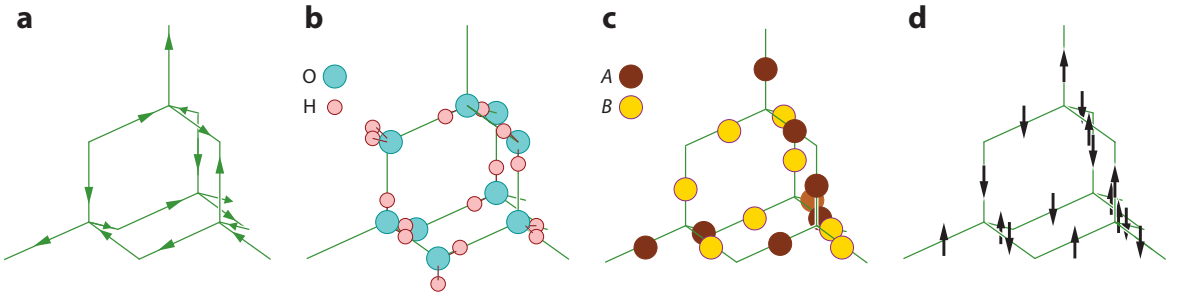

Figure 1

Mappings of the ice model on the diamond lattice (*green edges*). (*a*) Polarization arrows of the abstract ice model. (*b*) Water ice. (*c*) Compound of species *A* and *B*. (*d*) Ising ground state. Each configuration shown in parts *b*, *c*, and *d* maps to the arrow pattern in part *a*.

exactly the same ensemble. One realization is in oxides where the cations have a mix of two valence states, corresponding to species *A* and *B*; an example of this is magnetite Fe_3O_4, which has an equal mixture of Fe^{+2} and Fe^{+3} on the spinel "B" sublattice sites (20).

When $n = 1/2$, we can map the configurations to an ice model (**Figure 1*c***): each occupied site becomes an even-to-odd arrow on the corresponding bond of the parent lattice; each vacant site becomes a bond in the opposite direction (20). Another special filling is $n = 1/Z_B$, in which case we map the occupied sites to dimers.

2.3.1. Heavy-Electron Spinel LiV_2O_4. Another example is the metallic spinel LiV_2O_4 (21), which exhibits heavy-fermion behaviors despite the absence of *f* electrons. With ion charges Li^{+1} and O^{-2}, charge balance demands (on the vanadium-occupied B sites) $n = 1/2$ of V^{+3} and the rest of V^{+4}. Fulde and collaborators (21, 22) proposed quantum-mechanical models in which the correlated electrons can hop with amplitude *t* on the frustrated lattice.[2] They work from the limit of strong Coulomb repulsion, modeled discretely in the spirit of the Hubbard model; an on-site term effectively constrains the occupancy to, at most, one electron per site, plus the intersite repulsion *V*, which is responsible for the flux constraint.

2.4. Antiferromagnets

The remaining kinds of realization are magnetic.

2.4.1. Relation of antiferromagnetic Hamiltonian to constraint. Define $\mathbf{L}_\alpha$ to be the total spin on the cluster surrounding site α of the parent lattice (denoted by "$i \in \alpha$"):

$$\mathbf{L}_\alpha \equiv \sum_{i\in\alpha} \mathbf{s}_i. \qquad 2.1$$

We want the Hamiltonian to constrain

$$\mathbf{L}_\alpha = 0 \qquad 2.2$$

[2]The orbitals are actually *d* orbitals. Thus I have glossed over several complications of orbital degeneracy and orbital-dependent hopping amplitude, as well as spin.

for all α. Next, say the Hamiltonian can be written as

$$\mathcal{H}_{\text{spin}} = \frac{1}{2} J_{\text{spin}} \sum_{\alpha} \mathbf{L}_{\alpha}^{2}. \qquad 2.3.$$

Manifestly, this gives what we wanted: the classical ground states are any configuration satisfying Equation 2.2—the net spin in every cluster is zero. Furthermore, all such configurations are degenerate.

But in fact, if one simply expands the square in Equation 2.3, one gets an antiferromagnet with coupling $J_{ij} = J_{\text{spin}}$ if i and j belong to the same cluster, and zero otherwise. In the example lattices (all except the octahedral) where every cluster is a triangle or tetrahedron, that just means the nearest neighbors. *The ground states of the nearest-neighbor antiferromagnet are highly degenerate, but every state satisfies the constraint* (Equation 2.2) *around every* α.

The ground state ensemble of a system obeying constraints and lacking any kind of long-range order may in general be called a "cooperative paramagnet" (sometimes called "classical spin liquid," which means the same thing). It bears the same relation to the usual high-temperature paramagnetic state as the liquid bears to the gas state.

Next, I explain the three different situations in which antiferromagnets can form Coulomb phases (4).

2.4.2. Ising antiferromagnet. The ground states of the pyrochlore lattice Ising antiferromagnet have two up and two down spins in every tetrahedron. The Ising model is not realistic in its own right for three-dimensional lattices (mainly because their symmetry is incompatible with the special axis of the Ising spins), but many other models map to it. For example, the pyrochlore Ising antiferromagnet's ground states map 1-to-1 onto those of diamond-lattice ice model (20, 23). Each spin $t_i = +1(-1)$ maps to an arrow pointing along the corresponding diamond-lattice edge, in the positive (negative) sense from the even to the odd vertex. (See **Figure 1*d***.)

Notice that if we turn on an external field tuned to the appropriate size, the ground states (on any of our lattices) have $Z_{\mathcal{B}} - 1$ spins up and one down on every cluster; hence, this maps to a dimer covering.

2.4.3. Isotropic Heisenberg model: "classical spin liquid." This state arises when the spins are classical vectors (or can be treated as such), *if* all states in the continuous manifold satisfying Equation 2.2 are more or less equally likely. In this phase, every vector component of the spins satisfies the flux constraint; thus, the polarization field has indices not only for directions in space but also for the three spin components.

2.4.4. Isotropic Heisenberg model: "emergent discrete spins." This kind of state can arise in the classical models (mainly the triangle-based lattices) that manifest "order by disorder" in the sense of Moessner & Chalker (6, 7); it also arises in *all* quantum models with sufficiently large spin length S, when T is low enough that spin-wave energies favoring collinear or coplanar states are important (24–26). The spin-wave (free) energy has a local minimum in each discrete classical ground state that has all spins collinear (plus or minus) along the same axis; when the clusters are triangles (so there are no collinear ground

states), the local minimum states are the coplanar states. If calculated to sufficiently high order, the spin-wave (free) energy fully removes the degeneracy not due to symmetries, selecting a particular ordering pattern (for sure in the quantum case, and possibly in the classical case). However, quite often the latter terms in the selection (free) energy are much smaller than those favoring the discrete collinear/coplanar states. Hence, over an intermediate temperature range, the ensemble is well approximated using some sort of Ising model or coloring model of discrete states satisfying the constraint (Equation 2.2), and having a Coulomb-phase state.

2.5. Spin Ice

In the pyrochlore magnets $Dy_2Ti_2O_7$ and $Ho_2Ti_2O_7$, local $\langle 111 \rangle$ spin anisotropies (additional to Equation 2.3) reduce the ground-state manifold to effective Ising states (27, 28), as reviewed in Reference 29. The easy axis is the bond direction $\hat{\mathbf{u}}_i : \mathbf{s}_i = t_i \hat{\mathbf{u}}_i$ with $t_i = \pm 1$. The actual interactions are *ferromagnetic*: $J_F < 0$ but $\hat{\mathbf{u}}_m \cdot \hat{\mathbf{u}}_{m'} = -1/3$ for neighboring spins; thus the Hamiltonian in terms of $\{t_i\}$ reduces to an Ising model with *antiferromagnetic* $J = -J_F/3$. In terms of the original model, the ground states of this ensemble literally implement the ice rules, i.e., in each tetrahedron (surrounding a parent lattice node), two spins point in and two point out. Hence, these compounds are dubbed "spin ice."

2.5.1. Kagomé ice. When a (not too strong) magnetic field is placed on spin ice along (say) the [111] direction, it selects out a subset (still with extensive entropy) of ground states. Namely, every spin on a bond of the parent lattice in the [111] direction is parallel to the field. The three remaining sublattices are still free to fluctuate, but they form disconnected kagomé *layers*. Thus, we now have a stack of independent two-dimensional systems; hence this system (realized experimentally) is called "kagomé ice" (30). The parent lattice of each layer is a honeycomb lattice; the spin constraint in the layer is two in/one out on (say) the even nodes, and oppositely on the odd nodes. These configurations map exactly to those of a dimer model on the honeycomb lattice. (The dimer positions correspond to the single spin with its in/out sense opposite to the others in its triangle.)

2.5.2. Dipolar spin ice. The actual spin ice materials $Ho_2Ti_2O_7$ and $Dy_2Ti_2O_7$ are well approximated as having nothing but (long-ranged) *dipolar* spin interactions, rather than nearest-neighbor ones. Although this model is clearly related to the "Coulomb phase," I feel it is largely an independent paradigm with its own concepts that are different from the (entropic) Coulomb phase that most of this review is about.

The key fact is that all microstates satisfying the ice rules have very nearly the same energy (31, 32); this was first appreciated numerically [after some initial confusion, as it is tricky to simulate long-range interactions in periodic boxes (33)]. The simple explanation was given in Reference 34. It is a good approximation—for the far field, anyhow—to replace each point dipole by a pair (so-called "dumbbell") of opposite effective charges $\pm q$ having the same dipole moment μ, and we might as well separate them by the bond length d of the parent lattice (thus, $\mu = qd$). Then, all the effective charges sit on parent lattice nodes, and each node gets contributions from four dipoles (see **Figure 2**). Indeed, so long as the spin configuration satisfies the ice rules, those four contributions add to *zero* on *every* node, and (within this approximation) the interaction energy is zero. (I omitted a configuration-independent constant representing the interactions between the two charges

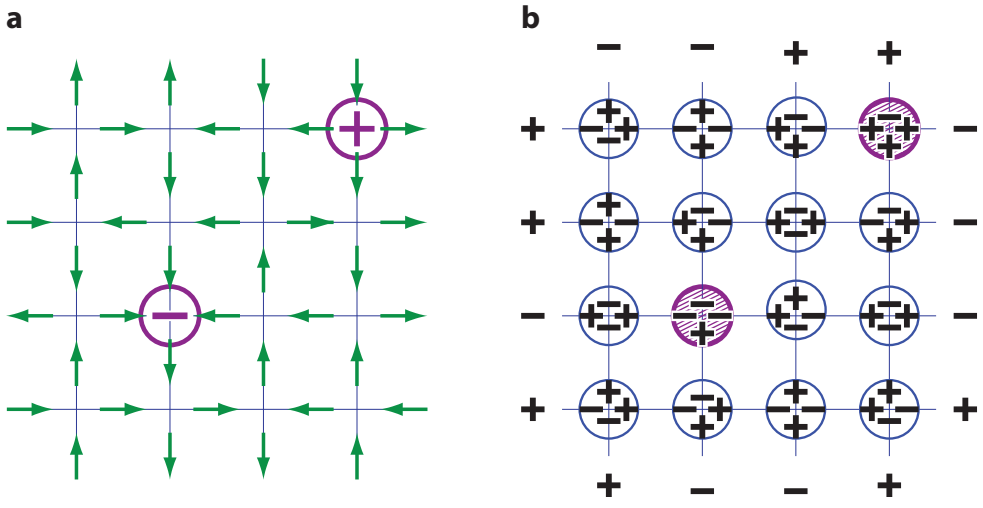

Figure 2

Dipolar spin ice and monopoles. (*a*) A configuration obeying ice rules, except for defects of charge $Q = +2$ and -2 (*circled plus and minus signs*). (*b*) When each dipole is replaced by a pair of charges (*+ and − symbols*) at the ends of its bond, these cancel out at every node of the parent lattice where the ice rule is obeyed (*open blue circles*), but add to a total proportional to Q at defect nodes (*shaded purple circles*).

forming each dipole.) In principle, small multipole interactions, representing the difference between the actual interactions of point dipoles and those of the effective charges, will break the degeneracy and lead to ordering at much lower temperatures.

3. COARSE-GRAINING, FOURIER MODE FLUCTUATIONS, AND LONG-RANGE CORRELATIONS

In this section, I present the steps leading to power-law correlations using the framework of a continuum theory, in which the ideas appear more transparently.

3.1. Polarization Field and Effective Free Energy

The polarization field is the key object of the Coulomb phase. As already laid out, our system has an extensive entropy of ground states (degenerate at this order). How do we handle this? Recall the discrete fluxes $\mathbf{P}_i$, which we defined along every bond of the parent lattice. Define a (whole-system) polarization density $\mathbf{P} \equiv \sum_i \mathbf{P}_i/\text{volume}$. It makes sense to write thermodynamic functions in terms of $\mathbf{P}$, because the ground-state entropy density evidently depends on it (the reasoning is elaborated in the next paragraph).

Recall the point of Section 1.2 that rearrangements (within the flux constraints) must occur along strings that follow flux arrows. On the one hand, if $\mathbf{P}$ is large, most fluxes have a positive component in that direction and the typical string crosses the system—a closed string would require half of its fluxes to have a backward component, but such a local gathering of reversed fluxes is unlikely. On the other hand, when $\mathbf{P}$ is near zero, there are many closed strings in any configuration, and hence many rearrangements that preserve $\mathbf{P}$. It is clear, then, that the number of configurations $\mathcal{N}(\mathbf{P})$ with a given polarization is

maximum at $\mathbf{P} = 0$ and goes to zero as $\mathbf{P}$ approaches its saturated value. Thus, let us define an entropy density

$$s(\mathbf{P}) \equiv \lim_{V\to\infty} \frac{\ln \mathcal{N}(\mathbf{P})}{V}, \tag{3.1.}$$

which is maximum at zero.

Next, so long as the ensemble is a "liquid" lacking long-range orders, the *local* polarization (if we divide the system into smaller boxes) is fluctuating, and not too strongly correlated from box to box. Then, the Central Limit Theorem says that the number of ground states for a given $\mathbf{P}$, in a system of large volume V, approaches a Gaussian form

$$\mathcal{N}(\mathbf{P}) \propto \exp(-|\mathbf{P}|^2/2{\sigma_P}^2) \tag{3.2.}$$

with a variance $\sigma_P^2 = 1/KV$ for some K. Comparing with Equation 3.1, we see that

$$s(\mathbf{P}) \approx s_0 - \frac{1}{2}K|\mathbf{P}|^2 \tag{3.3.}$$

for small $\mathbf{P}$. [All this was a completely standard argument from basic statistical mechanics; it is the same reason the free energy is proportional to (magnetization)^2 in a paramagnet, or that one assumes analyticity in the Landau free energy functional.]

Next, let us consider the spatial fluctuations of $\mathbf{P}$, which are more interesting (and more measurable!) than the functional form of $s(\mathbf{P})$. This requires defining a spatially varying polarization field $\mathbf{P}(\mathbf{r})$; it is a coarse-graining, i.e., the average of discrete polarizations over some neighborhood of $\mathbf{r}$ (one much larger than the lattice constant but much smaller than the system size). We assume $\mathbf{P}(\mathbf{r})$ varies smoothly. Corresponding to the discrete flux constraint, $\mathbf{P}(\mathbf{r})$ satisfies a divergence constraint

$$\nabla\cdot\mathbf{P}(\mathbf{r}) = 0, \tag{3.4.}$$

like a magnetic field without monopoles.

The total free energy (arising entirely from entropy) is the sum of those in the boxes or averaging volumes into which we can divide the system. Hence,

$$F_{\text{tot}}(\{\mathbf{P}(\mathbf{r})\})/T = \text{const} + \int d^d\mathbf{r}\frac{1}{2}K|\mathbf{P}(\mathbf{r})|^2. \tag{3.5.}$$

Equations 3.5 and 3.4, respectively, look like the field energy of a magnetic (or electric) field and its divergence constraint, in the absence of monopoles (or charges). That electrostatic (or magnetostatic) analogy is fruitful, and is why this state was dubbed "Coulomb phase."

In the case of dipolar spin ice, because the fluxes are parallel to real moments, the polarization is proportional to the real magnetization $\mathbf{M}$.

$$\mathbf{M} = \mu\mathbf{P}. \tag{3.6.}$$

Furthermore, if a region has a net polarization, we have a field energy of the form of Equation 3.5, but now $K \equiv \mu_0\,\mu^2$, where μ_0 is the permeability of free space, in the limit $T = 0$: it is purely energetic rather than entropic. At $T > 0$, the entropic elasticity gives a correction to the permeability. [In water ice, which has long-range electric dipole interactions, the analogous contribution to the dielectric constant has long been known (35).]

3.2. Pseudodipolar Correlations and Structure Factor

The standard way to evaluate correlations is to transform to Fourier space. Equation 3.4 gives

$$\mathbf{q}\cdot\mathbf{P}(\mathbf{q}) = 0; \tag{3.7.}$$

thus, Equation 3.5 gives

$$F_{\text{tot}} = \sum_{\mathbf{q}} \frac{1}{2} K |\mathbf{P}^{\perp}(\mathbf{q})|^2, \tag{3.8.}$$

where $\mathbf{P}^{\perp}(\mathbf{q})$ refers to the ("transverse") components of $\mathbf{P}(\mathbf{q})$ satisfying Equation 3.7. The fluctuations are gotten by first writing the (trivial) result of equipartition for an unrestricted $\mathbf{P}(\mathbf{q})$, and then projecting to obtain the transverse part:

$$\mathcal{S}_{\mu\nu}(\mathbf{q}) \equiv \langle P_{\mu}^{\perp}(-\mathbf{q}) P_{\nu}^{\perp}(\mathbf{q}')\rangle = \delta_{\mathbf{q},\mathbf{q}'} \frac{1}{K}\left(\delta_{\mu\nu} - \frac{q_\mu q_\nu}{|\mathbf{q}|^2}\right). \tag{3.9.}$$

3.2.1. Diffraction consequences. A physical observable $\Phi(\mathbf{r})$ usually has a contribution proportional to $\mathbf{P}$, but possibly the correspondence is modulated by, for example, alternating signs; if so, we write

$$\Phi_a(\mathbf{r}) = (\ldots) + \sum_{\mu} c_{a\mu}(\mathbf{r}) P_{\mu}(\mathbf{r}), \tag{3.10.}$$

where $\{c_{a\mu}(\mathbf{r})\}$ is a matrix of coefficients, with the symmetry of the lattice, and indices ab refer to possible components of the observable. It follows that the observable structure factor, measured in diffraction, behaves as[3]

$$\mathcal{S}^{\Phi}_{ab}(\mathbf{q}) \equiv \langle \tilde{\Phi}_a(\mathbf{q}) \tilde{\Phi}_b(-\mathbf{q})\rangle = (\ldots) + \sum_{\mu\nu\mathbf{Q}} f_{ab\mu\nu}(\mathbf{Q}) \mathcal{S}_{\mu\nu}(\mathbf{q}-\mathbf{Q}), \tag{3.11.}$$

where $f_{ab\mu\nu}(\mathbf{Q})$ is some sort of structure factor derived from the $c_{a\mu}$'s, and $\mathbf{Q}$ runs over reciprocal lattice vectors.

Two important features of diffraction may be noted, which were seen empirically in early simulations of the pyrochlore lattice (e.g., Reference 18), and already ascribed to the spin constraints by Moessner & Chalker (7). First, the polarization constraint says that a certain linear combination of fluxes is exactly zero (Moessner & Chalker's projection on the inward direction at a node of the parent lattice). That translates into a strict zero of the appropriate structure factor, at a certain wavevector. In the case of an antiferromagnet, or spin ice, the constraint is that magnetization is exactly zero in each cluster. Hence, we find a vanishing scattering near the zone center—the diffuse intensity grows as a high power of $|\mathbf{q}|$. [This is like the "hyperuniformity" property of certain off-lattice point patterns (36), meaning the structure factor vanishes at $\mathbf{q} = 0$.] Furthermore, the intensity has zeroes along every direction that is a symmetry axis of all clusters.

The second and more striking feature comes from the second term in Equation 3.9. Although not divergent, it is singular: the ratio has a different limit at $\mathbf{q} = 0$, depending on the direction of approach. In reciprocal space, this has the characteristic shape of a "pinch point," at which the contours of equal intensity have a roughly triangular shape. The form

[3]If "$(\ldots)$" in Equation 3.10 is a function of local fluctuating variables that has no conservation law, then "$(\ldots)$" in Equation 3.11 adds a nonsingular diffuse contribution on top of the features of $\mathcal{S}_{\mu\nu}(\mathbf{q})$.

factor in Equation 3.11 translates these to reciprocal lattice vectors **Q** other than zero, as seen in data from (37), shown in **Figure 3**. [Earlier experiments (38) gave less clear-cut images: polarized neutron diffraction is needed to separate the contributions from different spin components.]

I have discussed the way that other kinds of hard constraint also produce sharp features in reciprocal space (see Reference 4). For example, if you constrain a lattice gas on an fcc lattice so that every particle has an equal number of occupied neighbors, you get rings of diffuse scattering (39). [Similar features are observed in quasicrystals and ascribed to local tiling constraints (40). This constraint superficially resembles that of a Coulomb phase as laid out in Section 2.3; the outcome is different because the fcc lattice is not the medial lattice of a bipartite lattice.]

3.2.2. Real space correlations. Fourier transforming Equation 3.9 back to direct space gives

$$\langle P_\mu(0)P_\nu(\mathbf{r})\rangle \cong \frac{c_d}{Kr^d}\left(\delta_{\mu\nu} - d\hat{r}_\mu\,\hat{r}_\nu\right) \qquad 3.12.$$

at large separations $\mathbf{r}$ in d dimensions, where $\hat{\mathbf{r}} \equiv \mathbf{r}/|\mathbf{r}|$ and $c_3 = 4\pi$. Thus, the correlations, which one naively expected to be exponentially decaying in this "liquid-like" state, are instead power-law decaying, i.e., *critical*-like. They have the spatial dependence of a *dipole-dipole interaction*.

This criticality was appreciated in the ice model as early as 1973, being detected originally in a simulation (41). The universal explanation (above) of how dipolar correlations arise from Equation 3.5 with the divergence condition was first put forward

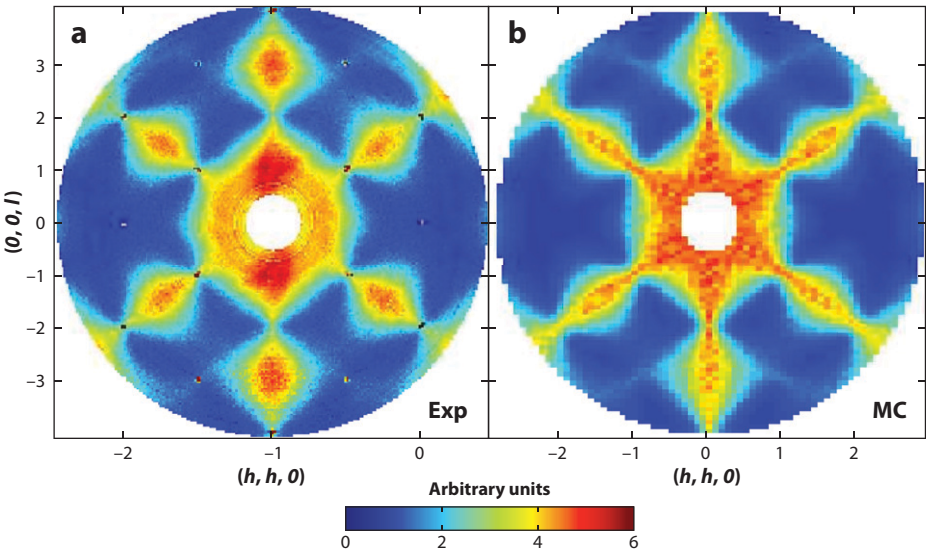

Figure 3

Pinch point in diffraction, after figures 2a,d of Reference 37. Spin-flip component of polarized neutron diffuse scattering from the spin-ice pyrochlore compound $Ho_2Ti_2O_7$, in the (h,h,l) plane of reciprocal space. (*a*) experimental result. (*b*) Monte Carlo simulation.

in 1981 to explain experiments on two-dimensional ice-like systems (2). It was noticed in the context of antiferromagnets in Reference 42 and (most influentially) announced as a general idea (initially for dimer coverings) by Huse et al. (3). Such correlations were verified by direct simulation in many models (e.g., References 3, 5, and 15).

We can apply these ideas to the nonlocal spin susceptibility near a defect. Consider a vector-spin antiferromagnet on one of the lattices in **Table 1**, where the spins are diluted (this corresponds to bond dilution on the parent lattice). At a dangling node, one that has just one neighbor, the flux constraint cannot possibly be satisfied. Such "orphan spins" respond to external fields just as free moments do. Using the Coulomb-phase framework, and in line with Equation 3.12 (or Equation 4.1 below) these spins' perturbation of the surrounding ones decays as a power law (with oscillations depending on how spins map to polarizations), as shown by Sen et al. (43), who explain NMR observations in $SrCr_{9p}Ga_{12-9p}O_{19}$ (following early hints given in section 4.4 of Reference 44).

3.2.3. Calculation for specific lattices. So far we only have obtained the asymptotic functional form near "pinch points." More practically, one would like to model (approximately) the diffuse scattering over the entire Brillouin zone for a specific model. For the spin models of Section 2.4, a systematic way is to allow $n \to \infty$ where n is the number of spin components. This "large-n" approach is a standard trick of statistical mechanics, useful because (in that limit) the constraint of unit length becomes irrelevant and we have a linear problem (5, 45, 46). The large-n formula turns out to be a good approximation even for $n = 1$.

An ad-hoc "maximum-likelihood" approach (4), which can be applied to *any* model of our class, is to consider the fluxes P_i (representing the model variables) to be *real* numbers, subject to two kinds of constraint: (*a*) that P_i take certain discrete values and (*b*) the usual divergence constraint. We then replace the first constraint *a* by a weighting $\exp(-\frac{1}{2}P_i^2/\sigma^2)$, where σ^2 is chosen to give the correct variance when the $\{P_i\}$ are chosen at random (and unconstrained by the divergence condition). For the spin models, this result (4) coincides with the large-n answer of Reference 5.

The third method for correlations is the cluster-variational approach (47), a mean-field theory that allows computation of nonlocal susceptibilities that can be converted to correlation functions. As this is built on tetrahedron units, it incorporates the constraint in the low-T limit and captures the pseudodipolar correlations; indeed, this result coincides with the other two (4), as $T \to 0$.

Finally, Villain & Schneider (48) predicted correlations in ice using a clever random-walk approximation to a series expansion, which has not yet been reconsidered in the literature. I would suspect this amounts to a Bethe-lattice approximation (i.e., neglecting the existence of loops in the lattice).

3.3. Height Models: Two-Dimensional Coulomb Phases

It is even easier to realize a flux constraint in $d = 2$ than in $d = 3$, and such models exhibit all the phenomena mentioned here. However, they exhibit additional, even more striking, behaviors that are peculiar to two dimensions and for that reason, they fall outside the scope of this review. Here, I just summarize the differences; such "height models" call for a review paper of their own.

To see what is different, recall that a divergence-free field such as our $\mathbf{P}(\mathbf{r})$ can always be written as a curl of a vector potential, $\mathbf{P}(\mathbf{r}) = \nabla \times \mathbf{A}(\mathbf{r})$. In three dimensions, $\mathbf{A}$ is ill defined

due to its gauge freedom; but in two dimensions, $A(\mathbf{r})$ has only one component (normal to the plane) and is an ordinary potential, uniquely defined modulo an additive constant. [To see this, note that $\mathbf{P}_{\rm rot} \equiv (-P_y, P_x)$ carries the same information as $\mathbf{P}$ but satisfies $\nabla \times \mathbf{P}_{\rm rot} = 0$; hence, $\mathbf{P}_{\rm rot} = \nabla A$ defines a potential.]

We can think of this as mapping a configuration of the variables to one of a crystal interface (49, 50) with profile $z = h(x, y) \equiv A(x, y)$. The "Coulomb phase" corresponds to the "rough" phase of such an interface model with the well-known form $F_{\rm tot} = \int d^2\mathbf{r} \frac{1}{2} K |\nabla h(\mathbf{r})|^2$. However, because $h(\mathbf{r})$ is uniquely defined, a generic physical variable (written in terms of field variables) is not only a linear combination of ∇h terms, but also has periodic terms of form $\cos(2\pi m h/a_\perp)$. [The repeat offset $a_\perp$ depends on the model and the definition of $h(\mathbf{r})$ (51–54).] The following can be shown:

1. This leads, in the rough phase, to critical correlations with a parameter- (and temperature-) dependent exponent $\propto T/K$.
2. An unroughening transition occurs when T/K decreases past a universal ratio, in which the system *locks* to a particular value of A, corresponding to *long-range order* of the model variables.
3. Thermally excited "defect charges" (see Section 4) do not necessarily destroy the critical phase; rather, they stay bound in pairs for T/K less than a universal critical ratio. The unbinding is the "Kosterlitz-Thouless" transition familiar in the XY model.

The critical correlations in point 1 imply singularities in reciprocal space, generally displaced at different positions in the Brillouin zone than the pinch points. Such singularities (in the height field) were called "zone-boundary singularities" in References 52–54 or (in the structure factor) "pi-ons" in Reference 55.

4. PSEUDO-CHARGE DEFECTS IN COULOMB PHASES

If we change our rules to allow configurations that violate the flux constraint, merely including a Hamiltonian that strongly penalizes the violations so they are dilute at low temperatures, what do we get? Such a defect may be labeled by its "charge" Q, equal to the net (nonzero) flux in the outward sense (at a parent-lattice vertex). This is a "charge" in the sense of Gauss's law, as the net flux through any surrounding surface must equal Q. That means the "charge" is conserved in time: the net charge in some volume cannot be changed except by moving it across the boundary, and defects can only be created in pairs of opposite charge. Their detectability from distant measurements, as well as the conservation properties, are characteristic of *topological defects*.

More interesting, in a Coulomb phase, the effective potential between defects must have the form of Coulomb's law:

$$F_{\rm int}(\mathbf{r}_1,\mathbf{r}_2)/T = \frac{KQ_1Q_2}{4\pi|\mathbf{r}_1 - \mathbf{r}_2|} \qquad 4.1.$$

(in $d = 3$). The interaction is defined by integrating the partition function, conditional that defect charges Q_1 and Q_2 are placed at $\mathbf{r}_1$ and $\mathbf{r}_2$, and by requiring the result to be proportional to $\exp(-F_{\rm int}/T)$. That is essentially how one obtains the Coulomb potential from the field energy in electro- or magnetostatics, and we must get the same result here, considering that the field free energy has exactly the same form. In $d = 3$ (but not necessarily in $d = 2$), our "charges" are *deconfined*, i.e., a defect/antidefect pair (in a large

system) will separate and have independent positions. By contrast, if these same defects are present in a phase with long-range order of the variables, pulling apart the defects now carries a cost proportional to $|\mathbf{r}_1 - \mathbf{r}_2|$: in that case, defects are "confined" the same way that quarks are.

Some authors have emphasized the notion of "Dirac string," meaning the trail of fluxes that got flipped as you pulled apart a defect/antidefect pair. It should be realized that this is a nebulous and not very helpful notion when applied in the Coulomb phase proper (with smallish polarization), for the string's path is not well defined. That is, there are many different, equally good ways to represent a defect pair by (*a*) taking some configuration from the undefected ensemble and (*b*) flipping the fluxes along a string. It is only in an ordered phase (see preceding paragraph), or near the limit of maximum polarization, that the Dirac string has a clear meaning.

When the model is a lattice gas of neighbor-repelling particles, and provided each particle maps to a dimer so as to form a dimer covering on the parent lattice, a simple way to create a defect/antidefect pair is to remove one particle or dimer (the total flux at the parent sites that the dimer spanned gets increased/decreased by the flux associated with a dimer). Evidently each of the two defects is carrying an effective particle number of 1/2, making this an elementary example of "fractionalization" (56).

In actual water ice, OH^- and H_3O^+ ions (if the hydrogen bond network is unbroken) are topological defects of charge $Q = \pm 2$ like the ones we were describing—except they are not very mobile, given that proton transfer is slow at icy temperatures. A distinct kind of defect, the Bjerrum defect, is formed when there are no protons, or two, along a given bond (maps to a nonmagnetic or doubly magnetic impurity in a spin system). The Bjerrum defects have charge $Q = \pm 1$ and are mobile.

4.1. Thermal Consequences

If the creation energy is E_Q for a defect of charge Q, the defect density will behave as $n_Q \propto \exp(-E_Q/T)$. The specific heat is affected proportionately. (As in semiconductors, the exponent is E_Q/T even though each defect pair costs $2E_Q$, due to entropy, as the defect locations are independent.)

The defect "charges" are in the same situation as ions in a plasma (or in water), or as carriers in a compensated semiconductor: we get Debye screening of the fields. In consequence, the "Coulomb" effective interaction, Equation 4.1, acquires a decaying factor $\exp(-\kappa|\mathbf{r}_1 - \mathbf{r}_2|)$, where $1/\kappa$ is the Debye screening length, given by

$$\kappa = \sqrt{\frac{n_Q K Q^2}{T}}. \qquad 4.2.$$

The pseudodipolar polarization correlations (Equation 3.12) acquire the same exponential screening factor. In Fourier space, this corresponds to replacing $|\mathbf{q}|^2 \to |\mathbf{q}|^2 + \kappa^2$ in the denominator of Equation 3.9.

How thermal excitation plays out in real systems depends on details of the model. In "spin ice," the spin configurations are not inherently constrained to obey the constraint; thus at $T > 0$, there is indeed a thermal concentration of defects. The cost

$$E_Q = \frac{1}{2} J Q^2 \qquad 4.3.$$

is $2J$ for the minimum charge $Q = \pm 2$. Following Equation 4.2, then, we expect $\kappa \propto \exp(-J/T)$, and this agrees with the experimental fit to the structure factor (37). Next, recall (from Section 3.2.1) the large basin in reciprocal space where the diffuse scattering was nearly zero, due to the exact cancellation in each tetrahedron, in the absence of defect excitations. Here, in the presence of thermal defects, we expect an increase of diffuse scattering $\propto n_Q \propto \exp(-2J/T)$ as is also observed (37).

Say one has a dimer model on a triangular lattice $\mathcal{L}$. This still is not a Coulomb phase (56), because the parent lattice is not bipartite. However, what if a very strong external strain field biases the dimer orientations such that one orientation is excluded? The lattice $\mathcal{L}'$ of retained bonds is a rhombic lattice, which *is* bipartite, and thus develops a Coulomb phase. Exactly the same thing happens in three dimensions with dimers on the fcc lattice (C.L. Henley, unpublished work).

For a final case, we once more disfavor a subset of dimer directions, but say the original lattice $\mathcal{L}$ was already bipartite (so the reduced lattice $\mathcal{L}'$ must be bipartite too). If the biasing field is strong but not infinite, what is the nature of the thermally excited defects consisting of dimers in "wrong" orientations? In the case of non-bipartite $\mathcal{L}$, they were effective charges in the polarization field $\mathbf{P}(\mathbf{r})$, but now they are merely dipoles. As we also know from electrostatics, an ensemble of dipoles changes the dielectric constant (or its analog $1/K$, in our case) but does not give Debye screening. Thus, even with some thermal excitations, we continue to see power-law correlations, so long as we still have a dimer-covering of a bipartite lattice. (The experimental example of "kagomé ice," where the external bias is the magnetic field, is similar: in that case, the bias causes a two-dimensional Coulomb phase to emerge from a three-dimensional one.)

4.2. "Magnetic Monopoles" in Dipolar Spin Ice

In the case of *dipolar* spin ice (recall Section 2.5.2), what happens at a node where the ice rules are violated, so the net flux there is Q? The same construction outlined in Section 2.5.2, whereby point dipoles get replaced by pairs of effective charges $\pm q$, must put a net (magnetic) charge of Q on every such defect node, just as it puts zero charge on every other node (see **Figure 2**). The total energy of such a microstate depends on the separations of all these defect charges by pairwise terms, each having a form like the Coulomb interaction: the defects are *emergent magnetic monopoles* (34).

We should be clear in what sense this is a monopole. Microscopically, of course, the laws of nature continue to rule out monopoles. Thus, near to any defect site, in between the bond directions where there is an excess of (say) outward flux, there must be other directions where there is a "counterflow" of inward flux. This seems rather analogous to the current associated with the Bogoliubov quasiparticle in a BCS superconductor. Its motion across the sample indeed causes a charge transport, proportional to the difference between the fractions of electron and hole making up the quasiparticle. Yet, while traveling in the bulk, the quasiparticle actually can have no charge (57) (in consequence, there, of the Meissner effect).

Notice that although the "charge" interactions in dipolar spin ice look formally like those in entropic Coulomb phases, the physics is quite different. In the entropic case, the *energy* cost is only the core cost of making the defects; the effective Coulomb interaction is wholly entropic, and emerges only as we allow the system in equilibrium to explore all

those many microstates. By contrast, in the dipolar case, *every* one of the (many) microstates having defects of $+Q$ and $-Q$ at $\mathbf{r}_1$ and $\mathbf{r}_2$ has very nearly the same spin interaction energy, dependent only on $|\mathbf{r}_1 - \mathbf{r}_2|$.

A way to note the difference is that for an ice model in $d = 2$, defect charges or monopoles separated by R feel a ln R potential in the entropic case (just consider Gauss's law for the model flux, confined to the plane), whereas in the dipolar case they have the usual $1/R$ interaction characteristic of three dimensions. Another situation that sharply illustrates the difference is "kagomé ice" (see Section 2.5.1). So long as the ice rules are satisfied, that system breaks up into decoupled two-dimensional layers. But when charge defects are introduced in the dipolar system, their interaction is isotropic—it is the same whether the two defects are in the same or in different layers (even though each defect is still free only to move within a layer). By contrast, in the kagomé ice phase of model spin ice with nearest-neighbor couplings, an interlayer defect interaction exists at all only to the extent that spins linking the layers have some fluctuations and mediate it.

Thus, one is tempted to reckon that the dipolar model, in which we have a bare magnetic energy, is trivial compared with short-range models, in which (entropic) Coulomb behavior emerges from a collective state. After all, our defect monopoles are not so different from the emergent monopoles found at the end of a long thin bar magnet, as we were taught in introductory magnetostatics. The important differences from bar magnet poles—and the reason for all the excitement—are that (*a*) our monopoles move freely in response to forces, (*b*) their magnetic charge is quantized (the quantized value depends on material properties), and (*c*) numerous cute experiments are possible that depend on the monopoles (58).

I would reserve the term "observation" of a monopole for an experiment isolating a single one. One might observe quantized jumps in the induced current around a conducting ring embedded in a sample whenever a monopole passes through it (34). Alternatively, a monopole just inside the sample's surface creates a characteristic $1/R$ field outside it, which might be detectable by a scanning magnetic force microscope.

The experiments done so far are one step less than this: they are thermodynamic and transport measurements, the interpretation of which requires monopoles to be the elementary excitations. Some of the experiments are

1. a phase separation between two paramagnetic phases—monopole liquid and monopole gas—as seen in kagomé ice (59);
2. magnetization dynamics (see Section 5.2 below), whereby the time derivative of magnetization maps to a monopole current (60);
3. how monopoles induced by temperature and magnetic fields modify the pseudodipolar correlations (37, 61, 62) (see Section 3.2 and 4.1);
4. and measuring the monopole charge by an analog of the Wien effect (63): that is, a magnetic field reduces the "ionization energy," which in turn increases the density of monopoles; this is manifested in a reduction of the spin autocorrelation time, as probed by muon spin relaxation (64).

It should be observed that many of the experiments basically probe the existence of thermally excited pseudo-charge defects, as could be found in any Coulomb-phase system; only a subset of the experiments test the special "monopole" property of the defects in the dipolar spin ice case (namely, their literal magnetostatic interaction).

4.2.1. Correlation length experiment. A recent experiment (61) on spin ice at high magnetic fields was interpreted in terms of monopoles. The polarization is near saturation; thus, the only freedom is in dilute line-like excitations, of overall density proportional to $\delta P = P_{\max} - P$. These are none other than the "world lines" of Section 7.4 below and also are genuine "Dirac strings;" if the flux constraint is absolute, they never terminate. But in the presence of a small density n of defects, each world line connects a defect and an antidefect (and all defects are endpoints), the typical length being P/n. (The connecting up is well-defined only to the extent that world lines do not touch, which is true if $(\Delta P)^2/n$ is sufficiently small.) The numerical agreement between the diffraction width and simulation results is indirect evidence for the finiteness of the Dirac strings, and hence for the presence of separated defects.

5. DYNAMICS

We could also make predictions for the dynamic fluctuations and response of the polarization field.

5.1. Accessibility of States Under Updates

As was pointed out (in Section 1.2), the natural update for a model with a flux is a loop update. (An example of such an update is shown in **Figure 4*a***.) However, with luck, one can run a simulation considering just minimal updates, i.e., involving the shortest loops (one plaquette, in the example of **Figure 4*a***, or a hexagon in the case that the parent lattice is a honeycomb or diamond lattice).

Now, to equilibrate a simulation, an update move must allow one to access every state with a given global flux, from every other state with the same flux, given enough steps. Minimal updates allow access in two-dimensional dimer models, but seem not to do so in the diamond-lattice dimer covering, so that nonlocal updates are needed. One method for this is a generalized "worm" update (65) (originally applied just to accelerate the dynamics

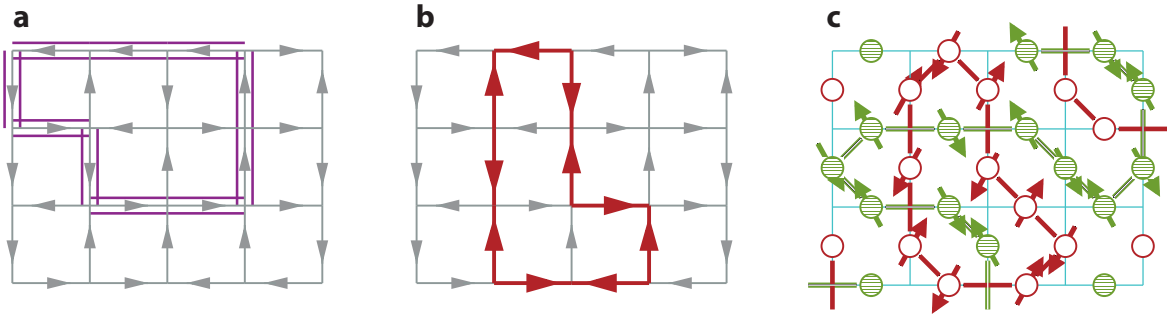

Figure 4

Loops in ice model and constrained disorder. (*a*) An ice-arrow configuration. Outlined is an update loop (reversing all arrows gives another valid configuration). (*b*) The same configuration; highlighted (*red arrows*) is an alternating loop (ice arrows point in alternating directions). (*c*) A lattice gas of A and B atoms (*red empty* and *green filled circles*) placed so that every vertex is surrounded by exactly two of each species, and represented by the same ice-arrow configuration as in part *a*. (Each red atom maps to an arrow from an even to an odd vertex, and oppositely for each green atom.) Bonds connecting atoms of the same species form alternating loops. Banks et al. (19) showed that for some plausible species-dependent couplings (in the three-dimensional analog), the spin directions alternate along each loop as shown.

in models for which minimal updates allow access). One creates a defect pair, allows the defects to diffuse until they reannihilate, and then accepts or rejects the final configuration according to the usual Metropolis fashion.

This is the typical mechanism for updating in a real system, too. That is, even rather dilute thermally excited defects are essential "lubricants" facilitating relaxation.

5.2. Dynamics of Defects

Topological defects, even when very dilute, may be crucial in the dynamic behavior for two reasons. First, the inherent dynamics of the Coulomb phase is presumably local, but a finite update may be insufficient to access all states in our ensemble. After all, as I have mentioned, the natural update follows a loop, and—given that the Coulomb phase has power-law correlations—one cannot rule out that the updating loops have a power-law distribution with a tail of long loops. But if a pair of defects is created, they then random-walk for a long time, and at last are reannihilated, this accomplishes the same effect as a long update loop. (If the trails of the defects never crossed—a big "if"—that loop would just be the joining of those trails.) The defect pair might be created by thermal activation in realistic dynamics, or artificially (as in the worm update) as a recipe to accelerate some Monte Carlo dynamics.

Defects matter for a second reason in cases such as spin ice or water ice, where the model polarization is a *physical polarization* (such as magnetization or electric polarization) that couples to external fields: they control the relaxation of the polarization. Let us consider spin ice for concreteness, and let $T > 0$, so there is some density $n(T)$ of thermally excited monopoles.

Whenever a monopole (defect) moves by $\Delta\mathbf{r}$, it changes the system's total polarization by $\Delta\mathbf{P}_{\text{tot}} = Q\Delta\mathbf{r}$. Firstly, this implies the relaxation rate of the total polarization is the monopole current,

$$\frac{d\mathbf{P}_{\text{tot}}}{dt} = \mathbf{J}_{\text{mono}}. \qquad 5.1.$$

Secondly, it implies the external (real) magnetic field $\mathbf{B}$ applies a force

$$\mathbf{F}_{\mathbf{B}} = Q\mathbf{B} \qquad 5.2.$$

on each monopole defect. Therefore, assuming a linear response with a mobility coefficient μ_{drift}, each defect has a drift velocity $\mu_{\text{drift}}Q\mathbf{B}$. Finally, the system's total magnetization is $\mu\mathbf{P}_{\text{tot}}$ (recall Equation 3.6). Putting it all together, the magnetization density behaves as

$$\frac{d\mathbf{M}_{\text{tot}}}{dt} = n(T)\mu_{\text{drift}}Q\mathbf{B}. \qquad 5.3.$$

(A stochastic term is omitted.) This apparently explains (60) the temperature dependences of the relaxation times observed years ago by Snyder et al. (66).

A slab of ideal spin ice, placed in a magnetic field, responds (at least in simulations) just like a slab of conductor placed in an electric field. After an initial current, surface charge layers form that nullify the field in the interior, and the current comes to a halt (60).

The nonequilibrium recombination dynamics of monopole defects with antidefects after a sudden quench is worked out by Castelnovo et al. (67), who suggest its use in real experiments.

5.3. Wavevector (In)Dependent Dynamics

Imagine first that the dynamics takes us between states that all exactly obey the zero-divergence constraint on $\mathbf{P}(\mathbf{r})$. Then, the dynamics of $\mathbf{P}$ is diffusive and standard dynamics would say

$$\frac{\partial \tilde{\mathbf{P}}_\perp(\mathbf{k})}{\partial t} = -\Gamma(\mathbf{k}) \frac{\delta F_{\text{tot}}}{\delta \tilde{\mathbf{P}}_\perp(\mathbf{k})} + \zeta(\mathbf{k}, t) \quad 5.4.$$

$$= \Gamma(\mathbf{k}) K \tilde{\mathbf{P}}_\perp(\mathbf{k}) + \zeta(\mathbf{k}, t). \quad 5.5.$$

I wrote the kinetic coefficient as "$\Gamma(\mathbf{k})$" to allow for different versions of the relaxational dynamics; $\zeta(\mathbf{k}, t)$ is a Gaussian noise source with correlation function $2T\Gamma(\mathbf{k})$, which satisfies detailed balance, and thus ensures that the steady state is the Boltzmann distribution implied by Equation 3.5. Hence, we get a relaxation time $\tau_0^{-1}(\mathbf{k}) = \Gamma(\mathbf{k})K$.

The naive expectation (4) is that, because the dynamics conserves polarization, $\tau_0^{-1} \propto \Gamma(\mathbf{k}) \propto |\mathbf{k}|^2$, vanishing at small $\mathbf{k}$. (That is the location of the static pinch-point singularities; when the actual variables measured are related to $\mathbf{P}$ by a staggering, the singularities get offset to other wavevectors $\mathbf{K}$.) However, for a vector-spin model, explicit analytic calculation (with a spin-conserving dynamic extension of the large-n approximation) and simulations (with realistic precessional dynamics) gave, according to Reference 68, a $\mathbf{k}$-independent relaxation, i.e., apparently $\Gamma(\mathbf{k}) \sim$ constant.

This is not the full story. At $T > 0$, the flux constraint is not fully satisfied; thus, there is a finite correlation length κ^{-1} (exponential in $1/T$, for a discrete model, or $\kappa(T)^2 \propto T$ in a vector-spin model), as mentioned above (see Equation 4.2). Conlon & Chalker (68) found a second contribution to the relaxation rate, $\tau_T(T)$, which represents a current of thermally excited monopoles [or the analogous excitations in a vector-spin model (68)]. The combined formula for the polarization correlations is (68)

$$\langle P_\mu(\mathbf{k}, t) P_\nu(-\mathbf{k}, 0) \rangle \propto \left(\delta_{\mu\nu} - \frac{k_\mu k_\nu}{|\mathbf{k}|^2} \right) e^{-t/\tau_T} \quad 5.6.$$

$$+ \kappa^2 \frac{k_\mu k_\nu}{|\mathbf{k}|^2 (|\mathbf{k}|^2 + \kappa^2)} e^{[1/\tau_0(\mathbf{k}) + 1/\tau_T]t}. \quad 5.7.$$

6. QUANTUM MODELS: A QUEST FOR "ARTIFICIAL LIGHT"

It is natural to ask whether we can have, not just an emergent magnetostatics or electrostatics, but an emergent *electrodynamics* with separate "electric" and "magnetic" fields satisfying Maxwell's equations (3, 69). Indeed, this can emerge in quantum versions of the models we have discussed (11, 70, 71).

6.1. Setup of Quantum Models

Typically, the Hilbert space consists of discrete configurations satisfying the same constraints we discussed before, allowing the definition of a "magnetic" field via the same coarse-graining developed in Section 3. Furthermore, the model has "flip" terms of amplitude t_{ring}, which hop you from one basis state to another. These are the same kinds of

"flips" (constrained by the flux conservation) we found in the classical (Monte Carlo, or physical) dynamics. (See Section 1.2. The flip must rearrange a closed loop.)

In a quantum model, it is particularly desirable that the "flip" look as simple as possible (at least, should be finite!) when written out in terms of spin or creation/annihilation operators. (Among other things, only the simpler cases are likely to be realized in experimental systems.) A "simple" flip means a "minimal update," which (in the quantum model) amounts to some variety of "ring exchange." That is, it switches the occupancies, or reverses the spins or arrows, along the shortest loops in the lattice. (These are six sites in the cases of the kagomé or pyrochlore site lattices.)

A natural route to the needed flip terms is to let the Hilbert space admit local violations of the flux constraint, but to make the Hamiltonian strongly penalize them by a potential energy cost of order V. The Hamiltonian also includes simpler flips of amplitude t_{pair} involving two sites (spin exchange or boson hopping). Then, a good effective Hamiltonian (low-energy theory) restricts the Hilbert space to the subset of configurations satisfying the flux constraint, but includes loop flip terms generated from perturbation theory (11, 71, 72), such as

$$t_{\text{ring}} \propto t_{\text{pair}}^3 / V^2 \qquad 6.1.$$

for loops of length six.

6.2. Theory of the "Maxwell" Phase

This theory, written in terms of discrete variables, is some kind of "compact $U(1)$ gauge theory." Here $U(1)$ simply means there is one sort of "electric" charge. It is the electric flux that has the defining constraint I mentioned in Section 1, which implies a gauge freedom in the phases of the electric field operators. Also, "compact" means the flipping term looks like $\cos(\Phi_B)$, where Φ_B plays the role of the *magnetic* flux, and thus the magnetic flux is only defined modulo 2π instead of taking arbitrarily large values. (In some papers, the role of "electric" and "magnetic" are flipped; there is not a uniform convention whether the variables are electric field operators.)

Now, let us assume the Φ_B fluctuations are rather small.[4] Then, events ("instantons") in the quantum evolution in which Φ_B wraps around its period get suppressed, maybe so much that we may ignore them, in which case we can imagine Φ_B being noncompact (taking unbounded values) as in the familiar electrodynamics. The next step is usually a leap to a continuum theory, by substituting for the "magnetic" (flip) term, the simplest analytic (i.e., quadratic) term with the correct symmetries, with a coefficient K_B (analogous to the magnetic permeability); also, a quadratic "electric" term is assumed as in the classical model. If all that is justified, it follows that we get emergent "artificial light": elementary excitations (11, 71) with dispersion

$$\hbar\omega(\mathbf{q}) = \hbar c|\mathbf{q}|, \qquad 6.2.$$

where $\hbar c \propto \sqrt{K_B/K_E}$ is the analog of the speed of light. Although linear dispersing excitations are common enough in solid state (magnons in antiferromagnets, or phonons), these

[4]Given that **E** and **B** operators are conjugate, like the position and momentum of a harmonic oscillator, the uncertainty relation tells us the "magnetic" fluctuations can be small only when the "electric" fluctuations are large, as is the case in the sort of correlated-liquid/cooperative-paramagnet phase we have had in mind throughout this review.

"emergent photons" are novel in that they are not Goldstone modes. I call such a phase a "Maxwell" phase.

The structure factors of such a model do have singularities at the same pinch points as the classical models, but the correlation behavior has different exponents. A shortcut to the behavior (as in any other model that reduces to harmonic oscillators) is the virial theorem, which says the oscillators' "potential" and "kinetic" energy expectations each get half the zero-point energy. Thus,

$$\left\langle \frac{K_E}{2} |\tilde{\mathbf{E}}(\mathbf{q})|^2 \right\rangle = 2(\hbar\omega(\mathbf{q})/4) \qquad 6.3.$$

(the 2 is for two polarizations). The equal-time mode expectations are thus (in place of the classical result (Equation 3.9)

$$\mathcal{S}_E(\mathbf{q}) \equiv \langle \tilde{\mathbf{E}}(\mathbf{q})_\alpha^* \tilde{\mathbf{E}}(\mathbf{q})_\beta \rangle \approx \frac{\hbar|\mathbf{q}|}{\sqrt{K_E K_B}} (\delta_{\alpha\beta} - \hat{\mathbf{k}}_\alpha \hat{\mathbf{k}}_\beta), \qquad 6.4.$$

and correspondingly the correlations should decay as $1/r^4$ in the quantum case. [The structure factor as a function of $(\mathbf{q}, \omega)$ is similar but proportional (71) to $|\mathbf{q}|^2/(\omega^2 + c^2|\mathbf{q}|^2)$ in place of the $|\mathbf{q}|$ factor in Equation 6.4.]

I somewhat mistrust the leap to the continuum theory, if justified only by the symmetries of the "flip" operator. Consider the following: given a *classical* model with a *classical* flip dynamics, one can always devise a quantum Hamiltonian whose ground state has the same probability distribution as the (Boltzmann) weights of the classical model, via the Rokhsar-Kivelson (RK) construction (73–75). But usually the classical system generally has relaxational dynamics, so correspondingly (74) the quantum system has elementary excitations with $\omega \sim |\mathbf{q}|^2$ dispersion; alternatively, if the classical relaxation time is constant (as in the model summarized in Section 5.3), the quantum excitations are *gapped*.

A second worry is that, as already noted (Section 1.2), a rule that flips only the smallest loops is quite possibly insufficient to access the whole Hilbert space.

Läuchli et al. (76) numerically computed the structure factor for a Coulomb-phase model (and other dimer models) at the RK point, and saw the expected $\omega \sim |\mathbf{q}|^2$ dispersion crossing over (with increasing $|\mathbf{q}|$) to a linear dispersion, which they interpret as a remnant of the artificial photons that would be present in a nearby "Maxwell phase."

6.3. Simulation Tests for Emergent Electrodynamics

Two groups have verified the emergent "Maxwell phase" (72, 77). Their models are dimer coverings of the diamond lattice (in the case of Reference 72, an equivalent boson model, in which the flip term is generated as in Equation 6.1). The "smoking gun" for this state, according to Reference 72, is correlations linear in $\mathbf{q}$, as in Equation 6.2; whereas for Reference 77, it is that constraining the flux density to $\mathbf{E}$ gives a total energy scaling as $|\mathbf{E}|^2$. Unfortunately, with quantum Monte Carlo it would be difficult to measure the corresponding dependences for the conjugate variable $\mathbf{B}$, which ought to behave the same as $\mathbf{E}$.

7. PHASE TRANSITIONS OUT OF COULOMB PHASES

Now that we have (in the polarization field) something analogous to an order parameter, we are equipped at least to classify transitions out of a Coulomb phase into, say,

a long-range-ordered phase. We might even be able to set up a field theory as the basis for some sort of renormalization group. But the constraints of the Coulomb phase necessarily mediate long-range interactions. As is long known (78), sufficiently long-ranged couplings will change the universality class of a transition, modifying the critical behavior to that characteristic of a higher spatial dimension.

The long-range-ordered pattern is a particular configuration. Therefore, it has a net polarization $\mathbf{P}_0$, which can be used to classify transitions into the following cases:

1. zero-polarization: the transition is a symmetry breaking into one of several symmetry-related states, all with $\mathbf{P}_0 = 0$,
2. intermediate polarization: $\mathbf{P}_0 \neq 0$, so there are several symmetry-related directions for $\mathbf{P}_0$, but each corresponds to just one kind of ordered state, and
3. saturated polarization: $\mathbf{P}_0 \neq 0$, with a symmetry breaking as in the previous case, but with $\mathbf{P}_0$ at the edge of the range of possible polarizations, so that there are no fluctuations whatsoever in the ordered state (so long as the constraint still holds).

Furthermore, such transitions might be driven either by pairwise interactions, or by external fields.

7.1. Dimer Crystal Transitions: Zero Polarization

The most elementary case is simulated dimer coverings of a cubic lattice, with an interaction that favors dimers to be on opposite sides of a square plaquette. [In $d = 2$, on a square lattice, that would induce the same columnar pattern found in quantum dimer models (79).] The ground state of this Hamiltonian is a periodic pattern having $\mathbf{P} = 0$ and with a six-fold degeneracy (three directions the dimers could line up in, and two choices of which layer to have dimers).

Simulations of this model by Alet et al. (80) showed a *continuous* transition from Coulomb phase to ordered phase (whereas Landau theory would predict a first-order transition, or an intermediate disordered phase). Furthermore, an emergent $SO(3)$ symmetry was seen in polarization space (by plotting the distribution of polarizations), but only right at the transition (81). These properties are suggestive of the recent paradigm of "deconfined" criticality (82, 83) whereby some phase transitions that must be first order according to Landau's picture, instead are continuous, and the critical state possesses an emergent symmetry lacking in either of the adjacent phases. A flurry (still unresolved) ensued of theories (84–87) and of follow-up simulations (87, 88).[5]

Reference 87 simulated less isotropic versions of the interaction Hamiltonian. The basic picture of the transition is that, coming from the high-temperature (Coulomb gas) phase, *all* of these cases belong to the same universality class, an inverted XY transition. Those free energy terms anisotropic with respect to the polarization direction are irrelevant at the critical fixed point; hence, the critical state has the $SO(3)$ symmetry, but they are relevant at the attracting fixed point characterizing the ordered phase. Thus, the transitions are less exotic than in the isotropic case but in one case, a surprising phase diagram was found: as temperature was raised, the dimer crystal melted into a paramagnetic phase, then at a

[5]Before the simulations mentioned, Bergman et al. (101) had pondered the transition from the Coulomb phase to an ordered dimer pattern with zero polarization. They concluded it is equivalent to the ordering of a superconductor when electromagnetic field fluctuations are taken into account, which is supposed to be weakly first order.

higher temperature, entered a Coulomb phase—re-entrant, in the sense that it has longer range correlations. (Notice that even if flux constraints are not enforced in the microstates, they may appear emergently.)

Papanikolaou & Betouras (88) elaborated the basic dimer model in a different way by including further neighbor interactions. They found a multicritical point (i.e., the transition switches from continuous to first order) not so far away from the basic model simulated by Alet et al. (80).

Chalker and Powell (85, 86) applied the world-line mapping (see Section 7.4) to this problem and massaged the result into a field theory with two complex fields. The symmetries related to the specific lattice imply that the terms in this field theory are either $SU(2)$ invariant, or of order 8 (hence, possibly irrelevant). This makes plausible the observed $SO(3)$ [equivalently $SU(2)$] symmetry at the transition, which goes with the "noncompact CP^1" ($NCCP^1$) universality class.

7.2. Intermediate Polarization Transitions

Whenever $\mathbf{P}_0 \neq 0$ (and is sufficient to label the symmetry-broken states), it should be possible to describe the transition just in terms of $\mathbf{P}(\mathbf{r})$ and its derivatives. If $\mathbf{P}_0$ is not saturated, the prescription of Landau theory should lead us more or less in the right direction: the free energy density $f(\mathbf{P})$ retains the full symmetry of the lattice, is analytic in $\mathbf{P}$, and has global minima at the $\mathbf{P}_0$ values. Furthermore, rather than compute the exact $f(\mathbf{P})$, we can usually get away with Taylor expanding it to the lowest order that has minima in the right places. For example, for ordering into a state with $\mathbf{P}_0$ in one of the six $\langle 111 \rangle$ directions, we might have

$$f(\mathbf{P}) = -\frac{1}{2}\alpha|\mathbf{P}|^2 + \frac{1}{4}\beta|\mathbf{P}|^4 - \nu(P_x^2 + P_y^2 + P_z^2) + \frac{1}{2}\gamma|\nabla\mathbf{P}|^2 \qquad 7.1.$$

When α, β, ν γ are all positive, the first two terms in Equation 7.1 define a minimum along the entire sphere $|\mathbf{P}|^2 = \alpha/\beta$; around that sphere, the third term is minimized when $\mathbf{P}$ points in any of the $\langle 100 \rangle$ directions. The gradient term puts a cost on the domain wall between ordered domains that have chosen different ones of the six $\mathbf{P}_0$ directions. So far, this looks exactly like the Landau-Ginzburg-Wilson "action" used to formulate the ε-expansion renormalization group for a three-component ferromagnetic spin model with cubic anisotropy (89). However, we are not done. If the flux constraint continues to hold through this transition, we must enforce $\nabla \cdot \mathbf{P} = 0$ in the continuum treatment. We saw in Section 3 that this constraint generates effective dipolar interactions betwen polarization fluctuations in different places, and such long-range interactions were shown long ago to change the critical behavior of spin models.

The case of nonzero, but unsaturated, polarizations has the fewest exotic features. It is realized by a Hamiltonian in which some bond directions are slightly strengthened, thereby selecting out a unique ground state (modulo spin-rotation symmetry), so the system undergoes a Néel transition. As might be expected, it behaves like the ordering of a vector-spin system with power-law interactions. In the vector-spin cases, this is slightly different from the related models studied in the 1970s (78), as the polarization field carries both spatial and spin component indices: the interaction is anisotropic (dipole-like) with respect to the former, but retains the rotation symmetry of the latter.

7.3. Saturated Polarization Case

This case has the further complication that, by the rules of our constraint, no fluctuations are possible at all on the ordered side of the transition. We thus get the asymmetric behavior called a "Kasteleyn transition" (90–92). On the one hand, approaching it from the ordered side, there are no critical divergences to signal the impending transition: in that sense, it looks like a first-order transition. On the other hand, coming from the Coulomb-phase side, fluctuations are allowed and in fact have critical divergences, as one would expect from a continuous transition. Finally, states near to the ordered, saturated state can be expressed relative to it as a set of dilute string excitations (see Section 7.4), and that typically implies a relatively tractable behavior. Kasteleyn transitions were studied experimentally in kagomé ice (two dimensions effectively) (93) and spin ice (61).

7.4. Mapping to $d - 1$ Quantum Problem: World-Line Approach

Here, I summarize a second analytic technique for Coulomb phases (beyond plain continuum theory of the polarization field), mapping a configuration in $d + 1$ dimensions to the world lines of a set of particles in d dimensions. Thus, one is taking advantage of the usual identity between the partition function of a $(d + 1)$-dimensional classical system and that of a corresponding d-dimensional quantum system, the latter appearing as a path integral in "imaginary time." The conservation law of these quantum particles corresponds to the defining divergence condition of the Coulomb-phase model.

The world-line mapping is ideally adapted to the case of a transition to a phase with saturated polarization (91)—that is, the limit in which the density of world lines goes to zero—but it was also applied to a zero-polarization case in References 85 and 86. This mapping has the disadvantage (compared to the polarization field theory) that it necessarily breaks the lattice symmetry by selecting one direction to be the (imaginary) time axis, along which the world lines run. The setup is detailed in the Appendix.

The Coulomb phase is the disordered phase of the world lines, which means that for every configuration found in the ensemble, you can find another configuration in which all the lines come out in the same place, except that two of them have gotten switched. Exactly as in the "entangled vortex liquid" phase, this signifies that the bosons in the $2 + 1$ dimensional quantum model are in a Bose-condensed phase—i.e., an ordered (!) phase with a continuous symmetry breaking labeled by one angle variable. Therefore, it has gapless Goldstone modes, the correlations of which decay as power laws in space and time. Furthermore, after one works through the mapping of dimer occupations to fluxes and of those, in turn, to the boson density and current, those power laws are precisely the dipolar correlations expected for the fluxes.

8. DISORDER

Coulomb-phase ideas can be applied to disordered cases—provided that the disorder does not destroy the Coulomb-phase nature of the state. If defects are very dilute, the basic phenomenology is that of the unchanged Coulomb phase between them, as discussed in earlier sections—in particular, the nonlocal spin response in Section 3.2.2. Similarly, disorder might create traps for pseudo-charge defects (Section 4), affecting their phenomenology much as impurity sites affect carriers in a compensated semiconductor. Here, I address examples of disorder that determine the collective state of the system.

8.1. Bond Disorder

One way to gently introduce disorder to a Coulomb phase is to weakly modulate the interactions in a nearest-neighbor antiferromagnet realization (say, the pyrochlore lattice), so the bond strength has variance $\tilde{\Delta}^2$ (94, 95). Standard replica techniques gave a mean-field spin glass transition temperature (95)

$$T_c^{\mathrm{MF}} = \frac{1}{2}\tilde{\Delta}\left(\lambda_4 \widehat{G^2}\right)^{1/2}, \qquad 8.1.$$

where $\lambda_4 = 6$ is a coefficient derived from the adjacency matrix, and $\widehat{G^2} \equiv \sum_j G_{ij}^2$, where G_{ij} is the correlation between spins i and j. Where Coulomb-phase notions enter is just in the evaluation of $\widehat{G^2}$. This has (thanks to our assumption of small $\tilde{\Delta}$) approximately the same numerical value as the pure case, for which we know the asymptotic behavior (Section 3.2), and indeed (within the large-N approximation) the exact function (45).

Alternatively, one considers *strong* random modulation, but in dilute places. This produces local pseudospin degrees of freedom, which have effective long-range interactions mediated by the polarization field (94, 95), as we know from Section 3 and Section 4. [These pseudospins are reminiscent of those that are induced at wrong bonds in an ordered antiferromagnet. The latter have pseudo-dipolar interactions mediated by the antiferromagnet's Goldstone mode (96).] Thus, the problem maps to a dipolar magnet dilutely occupied by spins, also giving a spin glass phase, as known for several decades.

8.2. Depleted Antiferromagnets

The "hyperkagomé" antiferromagnetic lattice (14, 15) is a pyrochlore lattice with one-quarter of the magnetic sites removed, making a very regular pattern of corner-sharing triangles. What if we dilute at random, but place the nonmagnetic substitutions such that exactly one site gets removed from every tetrahedron (97)? This ensemble is equivalent to the dimer coverings of the diamond lattice (where each dimer corresponds to a removed site), and thus is highly plausible as an example of a lattice-gas realization (see Section 2.3). The "flux" can still be defined, and is still conserved, on such "randomly depleted lattices." Hence, they still have Coulomb phases despite the disorder (97). The random disorder itself realizes a Coulomb-phase ensemble, and therefore it acts on the coarse-grained polarization field like a random anisotropy term with long-range dipolar-like correlations (97).

Uncorrelated site dilution creates occasional unsatisfied tetrahedra, which are pseudo-charges of the polarization field, as already discussed in Section 3.2.2.

8.3. Constrained Disorder Models: Loop-Based Dilution

There is an entire (nearly unstudied) class of correlated-disorder ensembles in which the frozen configurations come from some "Coulomb-phase" ensemble, for which I propose the name "constrained disorder." The depleted lattices are one example, and there are several others. In the rest of this section, I lay out one example introduced by Banks et al. (19).

In $CsNiCrF_6$ (18), A (=Cr) and B (=Ni) spins populate the pyrochlore such that every tetrahedron has two of each. (As noted in Section 2, this realizes an ice model.) The spin-spin exchange constants are J_{AA}, J_{AB}, and J_{BB}, depending on the species at either end of a bond. In a realistic range of couplings, the A spins in each tetrahedron point along $+\mathbf{n}$ and $-\mathbf{n}$, whereas the B spins point along an independent direction $+\mathbf{n}'$ and $-\mathbf{n}'$. Hence, the lattice breaks up into disjoint loops of A or B spins; in each loop, spin directions alternate, and each loop chooses a staggered direction independent of the others (**Figure 4*c***). Thus, the disorder-averaged spin correlation C_{ij} is simply the connectedness correlation function—the probability that sites i and j are on the same loop. In simulations (19), $C_{ij} \propto 1/r_{ij}^{a}$ with $a \cong 1$.

Consider flux-loops, as mentioned in Section 1.2, and also the basis of world lines in Section 7.4: flux runs in the same sense along the loop or line. One can make a one-to-one correspondence between configurations that have a flux-loop containing both sites $\mathbf{r}$ and $\mathbf{r}'$ to configurations with a charge defect at $\mathbf{r}$ and an antidefect at $\mathbf{r}'$. (Namely, one maps the former to the latter by reversing the flux along half the loop between $\mathbf{r}$ and $\mathbf{r}'$. For the reverse mapping, consider that any charge defect must be the endpoint of two such flux-lines; if the system has only one defect pair, the other endpoints must be at the second defect, so the map is invertible.) This idea—originating with Saleur & Duplantier (98)—was applied in two-dimensional height models to get the connectedness correlation function (51, 52, 99), and the same idea will work in Coulomb phases. However, the loops in question here are of a different kind: they run alternately with and against the flux. They cannot be reversed, so the defect-pair trick is not applicable. It will be interesting to see how a simple power law can emerge for the connectedness correlation function. The same kind of loops are formed by fermions in the wavefunctions envisaged by Fulde and colleagues (21, 22).

9. CONCLUSION

When local constraints imply the existence of a conserved "flux" in some statistical model, this flux can be coarse-grained into a polarization field that is a comprehensive framework—not yet exhausted—to map out the model's behaviors: long-range correlations, charge-like defects, dynamics, and disorder effects.

In the course of the review, I have outlined the associated calculational tools:

1. continuum theories, e.g., to model the analytic form of correlations in classical or quantum models;
2. the large-n limit of n-component spin models, to evaluate correlations in particular lattices; and
3. "world lines" (or equivalently "Dirac strings") near the limit of saturated polarization, e.g., the behavior of "spin ice" magnets in large fields of the appropriate orientations.

10. APPENDIX: SETUP OF WORLD-LINE MAPPING

Here, I present details of the world-line approach, applied to a variety of questions about Coulomb phases by Chalker and collaborators. The key idea is to map a configuration in

$d + 1$ dimensions to the world lines of a set of particles in d dimensions. Thus, one is taking advantage of the usual correspondence between the partition function of a $(d + 1)$-dimensional problem.

For pedagogical purposes, my illustrations are from the $1 + 1$ dimensional cases; although (as noted already in Section 3.3), these are "height" models and thus have much more structure than the $2 + 1$ dimensional Coulomb phase models. Specifically, the world lines in $1 + 1$ dimension are (usually) not crossing; so they represent hardcore bosons. In one dimension, one can reinterpret the particles (via a Jordan-Wigner transformation) as fermions, and the statistics naturally implements the hardcore constraint. (Furthermore, if a model has an exact solution, e.g., via the Bethe ansatz, the world-line picture is the way to set this up.) In $2 + 1$ dimensions, the fermion trick is not available: one is stuck with hardcore (thus, interacting) bosons. Given that one is mainly after long-wavelength properties, the repulsive interactions are not a big concern: one coarse-grains beyond the scale of the boson spacing, and describes the boson fluid using just (quantum) hydrodynamics.

Our mapping must ensure that the world lines do not turn back on themselves (so that the particles are conserved and do not annhilate). This is done by letting the world lines be the difference between the actual configuration and a reference configuration having saturated polarization in some reference direction. If the original configuration has a nonzero mean flux along the reference direction, the resulting array of world lines has a different density from the reference; whereas if the original flux is transverse, the resulting array becomes tilted, representing a nonzero current in the lower-dimensional quantum system.

Figure 5 illustrates two classes of this construction. **Figures 5*a–c*** show the "dimer-difference" construction. Quite generally, if you take two dimer coverings of the same lattice and fill in edges wherever they differ, you get a set of unbroken lines or loops. If one of the coverings has saturated flux in a certain direction, these lines are directed along that same direction. This construction was used in Reference 100.

I call the other construction a "uniform-flux construction"; this is implicit in the setup used by Powell & Chalker (85, 86). They define it for dimers on a simple-cubic lattice, which is oriented with the reference being the [111] axis; **Figures 5*d–f*** show the square lattice analog. The diagonal orientation of the world lines has the virtue that coordinate-axis directions remain symmetry equivalent. (Of course, one cannot manage that on other lattices, e.g. the honeycomb; if you wished the $\langle 111 \rangle$-type axes to remain equivalent, you would pick the [100] orientation for world lines.) In the uniform-flux construction, the flux-lines are not literally world lines, in that they can turn momentarily backwards in the odd layers; furthermore, each "particle" has two flux-lines that split apart. However, if one looks at the particles only in every fourth layer (dashed slices in **Figure 5*d***), the lines always move forwards in time (downwards in the figure) and always rejoin in the same pairs. In the simple cubic lattice, the slices should be taken every six layers, and each particle splits into three flux-lines, which will not always rejoin, but usually do. Rather than compute the exact transfer matrix eigenvalue $\lambda^6(q)$, Powell and Chalker just use a function with the same behavior near its maximum, for they are only interested in long-wavelength behaviors (and will get those by mapping the $d = 2 + 1$ problem to a field theory).

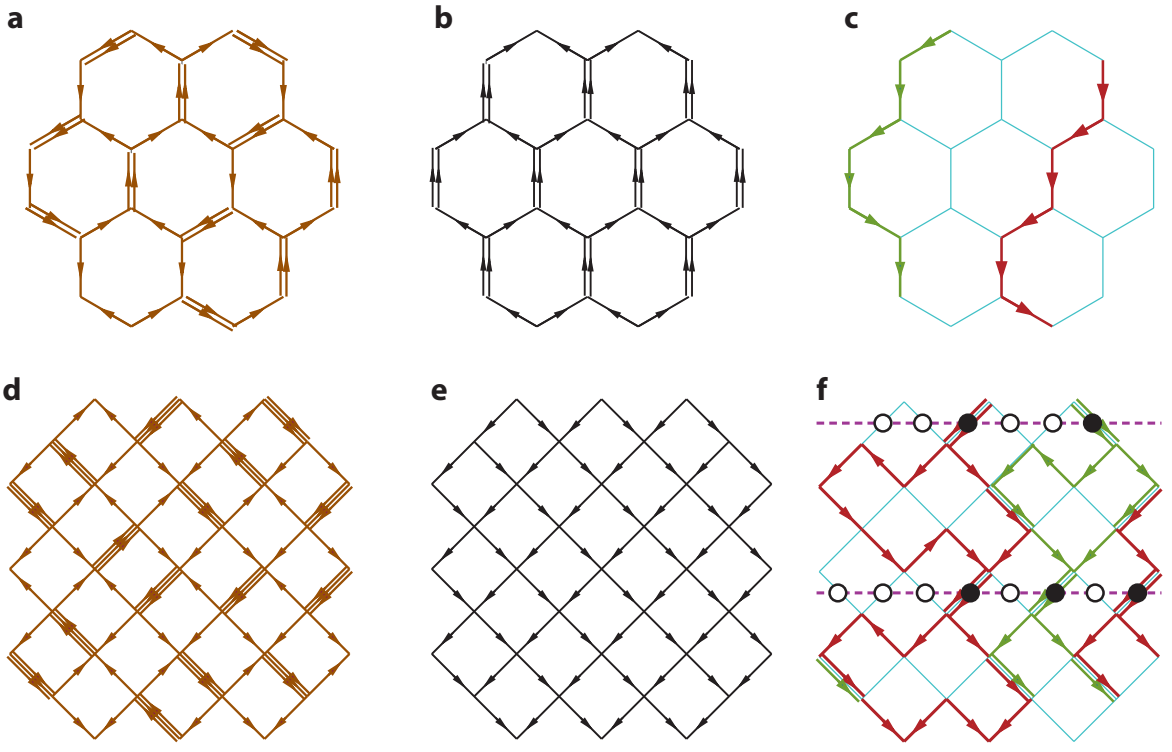

Figure 5

Mapping configurations of a flux model to world lines. Parts *a*, *b*, and *c* illustrate the dimer-difference construction. (*a*) A typical dimer covering on the honeycomb lattice, with arrows giving the fluxes; single arrows are uncovered edges. (*b*) A reference dimer covering, having the maximum possible flux (in the $+y$ direction). (*c*) The difference between the fluxes from parts *a* and *b* forms an array of nonintersecting lines that always move from top to bottom, and may thus be interpreted as world lines of a set of particles. Parts *d*, *e*, and *f* show the uniform-flux construction on the square lattice: again, part *d* is a typical dimer covering; part *e* is the reference flux pattern (but unlike part *b*, it does not represent any dimer covering); and part *f* is the difference, showing world lines. When we slice through every fourth layer of bonds (*purple dashed lines* in part *f*), the lines are always paired in that layer, and we interpret every pair as a particle (*filled circles*) in a chain of sites. (In parts *c* and *f*, all world lines are equivalent, but those that go with different particles are alternately colored red and green.)

DISCLOSURE STATEMENT

The author is not aware of any affiliations, memberships, funding, or financial holdings that might be perceived as affecting the objectivity of this review.

ACKNOWLEDGMENTS

I acknowledge helpful conversations and communications with Kedar Damle, Arnab Sen, Claudio Castelnovo, Roderich Moessner, Simon Banks, Nic Shannon, Frank Pollmann, Simon Trebst, Michel Gingras, and especially John Chalker. This work was supported by the NSF under grant DMR-0552461. I am grateful to Boston University for hospitality during the writing of this paper. I am grateful to Tom Fennell for producing **Figure 3**.

LITERATURE CITED

1. Ramirez AP. 1994. *Annu. Rev. Mater. Sci.* 24:453–80
2. Youngblood RW, Axe JD. 1981. *Phys. Rev. B* 23:232–38
3. Huse DA, Krauth W, Moessner R, Sondhi SL. 2003. *Phys. Rev. Lett.* 91:167004
4. Henley CL. 2005. *Phys. Rev. B* 71:014424
5. Isakov SV, Gregor K, Moessner R, Sondhi SL. 2004. *Phys. Rev. Lett.* 93:167204
6. Moessner R, Chalker JT. 1998. *Phys. Rev. Lett.* 80:2929–32
7. Moessner R, Chalker JT. 1998. *Phys. Rev. B* 58:12049–62
8. Siddharthan R, Georges A. 2002. *Phys. Rev. B* 65:014417
9. Lee S-H, Broholm C, Aeppli G, Perring TG, Hessen B, Taylor A. 1996. *Phys. Rev. Lett.* 76:4424–27
10. Chui ST. 1977. *Phys. Rev. B* 15:307–10
11. Hermele M, Fisher MPA, Balents L. 2004. *Phys. Rev. B* 69:064404
12. Pickles TS, Saunders TE, Chalker JT. 2008. *Europhys. Lett.* 84:36002
13. Petrenko OA, Paul DMcK. 2001. *Phys. Rev. B* 63:024409
14. Okamoto Y, Nohara M, Aruga-Katori H, Takagi H. 2007. *Phys. Rev. Lett.* 99:137207
15. Hopkinson JM, Isakov SV, Kee HY, Kim YB. *Phys. Rev. Lett.* 99:037201
16. Bernal JD, Fowler RH. 1933. *J. Chem. Phys.* 1:515–48
17. Pauling L. 1935. *J. Am. Chem. Soc.* 57:2680–84
18. Zinkin MP, Harris MJ, Zeiske T. 1997. *Phys. Rev. B* 56:11786
19. Banks ST, Bramwell ST, Fennell T, Harris MJ. 2010. Unpubl. manuscript
20. Anderson PW. 1956. *Phys. Rev.* 102:1008–13
21. Fulde P, Yaresko AN, Zyvyagin AA, Grin Y. 2001. *Europhys. Lett.* 54:779–85
22. Fulde P. 2004. *J. Phys. Condens. Matter* 16:S591–98
23. Liebmann R. 1986. *Statistical Physics of Periodically Frustrated Ising Systems (Lecture Notes in Physics)*, Vol. 251. Berlin/New York: Springer-Verlag. 141 pp.
24. Shender EF. 1982. *Sov. Phys. JETP* 56:178–84
25. Henley CL. 1989. *Phys. Rev. Lett.* 62:2056–59
26. Chalker JT, Holdsworth PCW, Shender EF. 1992. *Phys. Rev. Lett.* 68:855–58
27. Harris MJ, Bramwell ST, McMorrow DF, Zeiske T, Godfrey KW. 1997. *Phys. Rev. Lett.* 79:2554–57
28. Ramirez AP, Hayashi A, Cava RJ, Siddharthan R, Shastry BS. 1999. *Nature* 399:333–35
29. Bramwell ST, Gingras MJP. 2001. *Science* 294:1495–501; Bramwell ST, Gingras MJP. 2010. Spin ice state in frustrated magnetic pyrochlore materials. In *Introduction to Frustrated Magnetism: Materials, Experiments, Theory*, ed. C Lacroix, F Mila, P Mendels. *Springer Ser. Solid-State Sci.*, Vol. 164. Available Jan. 2, 2011 (arXiv:0903.2772)
30. Wills AS, Ballou R, Lacroix C. 2002. *J. Phys. Condens. Matter* 14:L559
31. Melko RG, Gingras MJP. 2004. *J. Phys. Condens. Matter* 16:R1277–319
32. Isakov SV, Moessner R, Sondhi SL. 2005. *Phys. Rev. Lett.* 95:217201
33. Siddharthan R, Shastry BS, Ramirez AP, Hayashi A, Cava RJ, Rosenkranz S. 1999. *Phys. Rev. Lett.* 84:3430
34. Castelnovo C, Moessner R, Sondhi SL. 2008. *Nature* 451:42–45
35. Nagle JF. 1974. *Chem. Phys.* 43:317–28
36. Torquato S, Stillinger FH. 2003. *Phys. Rev. E Stat. Nonlin. Soft Matter Phys.* 68:041113
37. Fennell T, Deen PP, Wildes AR, Schmalzl K, Prabhakaran D, et al. 2009. *Science* 326:415–17
38. Bramwell ST, Harris MJ, den Hertog BC, Gingras MJP, Gardner JS, et al. 2001. *Phys. Rev. Lett.* 87:047205
39. De Ridder R, van Tendeloo G, Amelinckx S. 1976. *Acta Crystallogr. A* 32:216–24
40. Henley CL. 1991. In *Quasicrystals: The State of the Art*, ed. PJ Steinhardt, DP DiVincenzo, pp. 429–524. Singapore: World Sci
41. Stillinger FH, Cotter MA. 1973. *J. Chem. Phys.* 58:2532–41

42. Henley CL. 1992. *Bull. Am. Phys. Soc.* 37:441–42
43. Sen A, Damle K, Moessner R. 2009. Unpubl. manuscript
44. Henley CL. 2001. *Can. J. Phys.* 79:1307–28
45. Garanin DA, Canals B. 1999. *Phys. Rev. B* 59:443–56
46. Canals B, Garanin DA. 2001. *Can. J. Phys.* 79:1323–31
47. Yoshida S, Nemoto K, Wada K. 2002. *J. Phys. Soc. Jpn.* 71:948–54
48. Villain J, Schneider J. 1973. In *Physics and Chemistry of Ice*, ed. E Whalley, SJ Jones, LW Gold, pp. 285–90. Ottawa: R. Soc. Can.; Villain J. 1972. *Solid State Commun.* 10:967–70
49. van Beijeren H. 1977. *Phys. Rev. Lett.* 38:993–96
50. Blöte HWJ, Hilhorst HJ. 1982. *J. Phys. A* 17:3559
51. Kondev J, Henley CL. 1996. *Nucl. Phys. B* 464:540–75
52. Kondev J, Henley CL. 1995. *Phys. Rev. B* 52:6628–39
53. Raghavan R, Henley CL, Arouh SL. 1997. *J. Stat. Phys.* 86:517–50
54. Zeng C, Henley CL. 1997. *Phys. Rev. B* 55:14935–47
55. Moessner R, Sondhi SL. 2003. *Phys. Rev. B* 68:064411
56. Moessner R, Sondhi SL. 2001. *Phys. Rev. Lett.* 86:1881–84
57. Kivelson SA, Rokhsar DS. 1990. *Phys. Rev. B* 41:11693
58. Castelnovo C. 2010. *ChemPhysChem* 11:557–59
59. Higashinaka R, Fukazawa H, Deguchi K, Maeno Y. 2004. *J. Phys. Soc. Jpn.*: 2851–56
60. Jaubert LDC, Holdsworth PCW. 2009. *Nat. Phys.* 5:258–61
61. Morris DJP, Tennant DA, Grigera SA, Klemke B, Castelnovo C, et al. 2009. *Science* 326:411–14
62. Kadowaki H, Doi N, Aoki Y, Tabata Y, Sato TJ, et al. 2009. *J. Phys. Soc. Jpn.* 78:103706
63. Sondhi SL. 2009. *Nature* 461:888–89
64. Bramwell ST, Giblin SR, Calder S, Aldus R, Prabhakaran D, Fennell T. 2009. *Nature* 461:956–60
65. Alet F, Sorensen E. 2003. *Phys. Rev. E Stat. Nonlin. Soft Matter Phys.* 67:015701
66. Snyder J, Ueland BG, Slusky JS, Karunadasa H, Cava RJ, Schiffer P. 2004. *Phys. Rev. B* 69:064414
67. Castelnovo C, Moessner R, Sondhi SL. 2010. *Phys. Rev. Lett.* 104:107201
68. Conlon PH, Chalker JT. 2009. *Phys. Rev. Lett.* 102:237206
69. Moessner R, Sondhi SL. 2003. *Phys. Rev. B* 68:184512
70. Balents L, Fisher MPA, Girvin SM. 2002. *Phys. Rev. B* 65:224412
71. Tewari S, Scarola VW, Senthil T, Das Sarma S. 2006. *Phys. Rev. Lett.* 97:200401
72. Banerjee A, Isakov SV, Damle K, Kim YB. 2008. *Phys. Rev. Lett.* 100:047208
73. Rokhsar DS, Kivelson SA. 1988. *Phys. Rev. Lett.* 61:2376–79
74. Henley CL. 2004. *J. Phys. Condens. Matter* 16:S891–98
75. Castelnovo C, Chamon C, Mudry C, Pujol P. 2005. *Ann. Phys. (NY)* 318:316–44
76. Läuchli AM, Capponi S, Assaad FF. 2008. *J. Stat. Mech.* 2008:01010
77. Sikora O, Pollmann F, Shannon N, Penc K, Fulde P. 2009. *Phys. Rev. Lett.* 103:247001
78. Fisher ME, Aharony A. 1973. *Phys. Rev. Lett.* 30:559–62; Aharony A. 1973. *Phys. Rev. B* 8:3363–70
79. Read N, Sachdev S. 1989. *Phys. Rev. Lett.* 62:1694–97
80. Alet F, Misguich G, Pasquier V, Moessner R, Jacobsen JL. 2006. *Phys. Rev. Lett.* 97:030403
81. Misguich G, Pasquier V, Alet F. 2008. *Phys. Rev. B* 78:100402
82. Senthil T, Vishwanath A, Balents L, Sachdev S, Fisher MPA. 2004. *Science* 303:1490–94
83. Balents L, Sachdev S. 2007. *Ann. Phys. (NY)* 322:2635–64
84. Charrier D, Alet F, Pujol P. 2008. *Phys. Rev. Lett.* 101:167205
85. Powell S, Chalker JT. 2008. *Phys. Rev. Lett.* 101:155702
86. Powell S, Chalker JT. 2009. *Phys. Rev. B* 80:134413
87. Chen G, Gukelberger J, Trebst S, Alet F, Balents L. 2009. *Phys. Rev. B* 80:045112
88. Papanikolaou S, Betouras JJ. 2010. *Phys. Rev. Lett.* 104:045701
89. Aharony A. 1973. *Phys. Rev. B* 8:4270–73

90. Nagle JF, Yokoi CSO, Bhattacharjee SM. 1989. Dimer models on anisotropic lattices. In *Phase Transitions and Critical Phenomena*, ed. C Domb, JL Lebowitz, 13:235–97. New York: Academic
91. Powell S, Chalker JT. 2008. *Phys. Rev. B* 78:024422
92. Jaubert LDC, Chalker JT, Holdsworth PCW, Moessner R. 2008. *Phys. Rev. Lett.* 100:067207
93. Fennell T, Bramwell ST, Manuel P, Wildes AR. 2007. *Nat. Phys.* 3:566–72
94. Saunders TE, Chalker JT. 2007. *Phys. Rev. Lett.* 98:157201
95. Andreanov A, Chalker JT, Saunders TE, Sherrington D. 2010. *Phys. Rev. B* 81:014406
96. Villain J. 1979. *Z. Phys. B* 33:31–42
97. Henley CL. 2009. *J. Phys.: Conf. Ser.* 145:012022
98. Saleur H, Duplantier D. 1987. *Phys. Rev. Lett.* 58:2325–28
99. Kondev J, Henley CL. 1995. *Phys. Rev. Lett.* 74:4580–83
100. Dhar A, Chaudhuri P, Dasgupta C. 2000. *Phys. Rev. B* 61:6227–37
101. Bergman DL, Fiete GA, Balents L. 2006. *Phys. Rev. B* 73:134402

Annual Review of Condensed Matter Physics

Volume 1, 2010

Contents

Errata

An online log of corrections to *Annual Review of Condensed Matter Physics* articles may be found at http://conmatphys.annualreviews.org/errata.shtml